Quaternary Science Reviews xxx (xxxx) xxx

Contents lists available at ScienceDirect

Quaternary Science Reviews

journal homepage: www.elsevier.com/locate/quascirev

A Neanderthal's specialised burning structure compatible with tar obtention

Juan Ochando [a,b,*], Francisco J. Jiménez-Espejo [c,d,**], Francisco Giles-Guzmán [e], Carlos Neto de Carvalho [f], Jose S. Carrión [a,g], Fernando Muñiz [h], Juan Manuel Rubiales [i], Pedro Cura [j,k], João Belo [k], Stewart Finlayson [e,l], Belen Martrat [m], Barend L. van Drooge [m], Gonzalo Jiménez-Moreno [n], Antonio García-Alix [n], Jose Antonio Lozano Rodríguez [o,p], Rosa María Albert [q,r], Naohiko Ohkouchi [d], Nanako Ogawa [d], Hisami Suga [d], Jon Camuera [c], Francisca Martínez-Ruiz [c], Joan Villanueva [s], Oriol Teruel [s], Nina Davtian [s], Noel Moreira [t], Zain Belaústegui [u], Joaquín Rodríguez-Vidal [e,v], Manuel Munuera [w], Alex Menez [e], Geraldine Finlayson [e,l,x], Clive Finlayson [e,l,x]

[a] Department of Plant Biology (Botany Area), Faculty of Biology, University of Murcia, Murcia, Spain
[b] Sapienza University of Rome, Department of Environmental Biology, Italy
[c] Instituto Andaluz de Ciencias de la Tierra (IACT), CSIC, Armilla, Spain
[d] Biogeochemistry Research Center, Research Institute for Marine Resources Utilization, Japan Agency for Marine-Earth Science and Technology, Yokosuka, Kanagawa, Japan
[e] The Gibraltar National Museum, Gibraltar
[f] Serviço de Geologia do Município de Idanha-a-Nova, UNESCO Naturtejo Global Geopark, Instituto D. Luiz, University of Lisbon, Portugal
[g] Evolutionary Studies Institute, University of Witwatersrand, South Africa
[h] Departamento de Cristalografía, Mineralogía y Química Agrícola, Universidad de Sevilla, Spain
[i] Departamento de Sistemas y Recursos Naturales. Escuela Técnica Superior de Ingeniería de Montes, Forestal y del Medio Natural. Universidad Politécnica de Madrid. Madrid, Spain
[j] Laboratório de Arqueologia Experimental, ITM - Instituto Terra e Memória, Centro de Estudos Superiores de Mação, Mação, Portugal
[k] CGEO—Geosciences Center, Universidade de Coimbra, Coimbra, Portugal
[l] The University of Gibraltar, Gibraltar National Museum Campus, Gibraltar
[m] Instituto de Diagnóstico Ambiental y Estudios del Agua (IDAEA), CSIC, Barcelona, Spain
[n] Departamento de Estratigrafía y Paleontología, Universidad de Granada, Spain
[o] Canary Islands Oceanographic Center (COC), Spanish Institute of Oceanography (IEO), Spanish Research Council (CSIC), Santa Cruz de Tenerife, Spain
[p] Departament of History and Philosophy, Prehistory Area, University of Alcalá, Alcalá de Henares, Spain
[q] Departament de Prehistoria. Autonomous University of Barcelona. Cerdanyola del Vallès, Spain
[r] ICREA, Barcelona, Spain
[s] Institute of Environmental Science and Technology, Autonomous University of Barcelona (ICTA-UAB). Cerdanyola del Vallès, Spain
[t] Instituto de Investigação e Formação Avançada (IIFA), University of Évora and Institute of Earth Sciences (ICT) - Pole of University of Évora, Portugal
[u] Departament de Dinàmica de la Terra i de l'Oceà, Facultat de Ciències de la Terra, Institut de Recerca de la Biodiversitat (IRBio), Universitat de Barcelona (UB), Spain
[v] Department of Earth Sciences, Faculty of Experimental Sciences, University of Huelva, Campus del Carmen, Huelva, Spain
[w] Department of Agricultural Engineering, Polytechnic University of Cartagena, Cartagena, Spain
[x] Department of Life Sciences, Liverpool John Moores University, Liverpool, United Kingdom

ARTICLE INFO

Handling editor: Claude Hillaire-Marcel

Keywords:
Neanderthals
Palaeolithic
Tar

ABSTRACT

Here we present multiproxy evidence of a new type of Neanderthal hearth discovered in Vanguard Cave (VC) (Gibraltar), which is dated ~ 65 kyr, and associated with Middle Paleolithic stone artefacts. The hearth structure coincides with predictions from theoretical studies which require the use of heating structures for obtaining birch tar, commonly used in hafting. We propose that the structure was used for heating rockroses (Cistaceae) under anoxic conditions by burning herbs and shrubs, over a guano mixed with sand layer. We tested this hypothesis

* Corresponding author. Department of Plant Biology (Botany Area), Faculty of Biology, University of Murcia, Murcia, Spain.
** Corresponding author. Instituto Andaluz de Ciencias de la Tierra (IACT), CSIC, Armilla, Spain.
E-mail addresses: juan.ochando@um.es (J. Ochando), francisco.jimenez@csic.es (F.J. Jiménez-Espejo).

https://doi.org/10.1016/j.quascirev.2024.109025
Received 8 August 2024; Received in revised form 22 October 2024; Accepted 22 October 2024

Palaeoecology
Geochemistry
Palynology
Retene
Gibraltar caves

experimentally with success. The presence of levoglucosan and retene in the structure's matrix points to combustion of higher resinous plant-derived material. Our results advance our understanding of Neanderthal behaviour, as the ability to organize activities related with the use of fire.

1. Introduction

Fire use and control would have provided crucial adaptive advantages to *Homo* (Brown et al., 2009), even have shaped its evolution (Wrangham, 2009; Sankararaman et al., 2014; Monge et al., 2015). Manufacturing fire technology has been shown common ever since 400 ka to present (e.g., Rosell and Blasco, 2019) and most likely, it happened long before (Wilkins et al., 2012). The ability to make, conserve, and transport fires by Neanderthals has been highlighted by different studies (e.g., Roebroeks and Villa, 2011). Function, characteristics and type of fire related to Neanderthals have been described (Grünberg, 2002; Mazza et al., 2006; Modugno et al., 2006; Boeda et al., 2008) although direct evidences are still scarce (Heyes et al., 2016; Sorensen et al., 2018; Rots et al., 2020). The main functions for the use of fire have been related to provide heat, light and the possibility of cooking food. However, it can also be connected to the development of new technological innovations. These may include intentional heat treatment of stone artefacts (Agam et al., 2021), enduring wood (Aranguren et al., 2018), smoking purposes (Vidal-Matutano and Théry-Parisot, 2016) and the production of multicomponent tools, hafting stone flakes in wooden elements, with the use of adhesives from birch bark distillation (Koller et al., 2001; Maza et al., 2006; Pawlik and Thissen, 2011; Niekus et al., 2019; Schmidt et al., 2024) and conifer resin (Degano et al., 2019). Other technological innovations attributed to Neanderthals are the construction of pits (Leierer et al., 2020) and the diversification of the fuel types used (Yravedra and Uzquiano, 2013) with different commonly used plants (Henry, 2017), liquid hydrocarbons (Courty et al., 2012) and lignites (Théry-Parisot and Meignen, 2000). Plants are, however, the most common type of fuel and it is therefore expected they have been subject to selection processes by Neanderthals among the available resources in the landscape, in the vicinity or perhaps beyond (Uzquiano, 2008; Thèry-Parisot, 2001; Allué et al., 2017; Henry, 2017; Vidal-Matutano et al., 2017).

In order to understand Neandethal's technological capacity we report the discovery of a complex hearth/sedimentary structure at Vanguard Cave (Gibraltar, Fig. 1), it will be called the "structure" along the manuscript. The structure that has revealed a hitherto unknown way by which Neanderthals managed and used fire. In order to reach the goal of understanding the purpose of the structure we complete an extensive multiparametric analysis, a logic inductive approach and results of a series of field experiments.

2. The site

2.1. Geographical location

Vanguard Cave (VC, 36 ° 7′ 17″ N, 5 ° 20′ 30″ W) is located at sea level on the promontory of Gibraltar in the south of the Iberian Peninsula (Fig. 1). Gibraltar is situated on the northern coast of the Strait of Gibraltar, which connects the Mediterranean Sea with the Atlantic Ocean. Several caves, including Vanguard, Gorham's, Bennett's, and Hyaena were occupied by Neanderthals and form part of the Gorham's Cave Complex UNESCO World Heritage Site (https://whc.unesco.org/en/list/1500). Geomorphological studies have shown that the Gibraltar Peninsula underwent important tectonic uplifts and eustatic sea-level fluctuations during the Pleistocene (Jiménez-Espejo et al., 2013; Rodríguez-Vidal et al., 2013). In this context, the deposits inside VC formed when the coastal shelf was emerged, with the coastline up to 4.5 km distant. The VC sand dune deposits were formed over a protracted period of MIS (Marine Isotopic Stage) 5d-to-3 interval (Jiménez-Espejo et al., 2013; Rodríguez-Vidal et al., 2013).

2.2. Stratigraphy

VC contains 17 m thick deposits, mainly composed of massive, coarse-to-medium sands intermixed with tabular-to-lenticular units of silts and silty sands (Macphail and Goldberg, 2000). In the upper excavation area of the cave - uppermost ~5m of the VC sequence - the sands are interdigitated with black humic clays, showing evidence of phosphatisation (Macphail et al., 2013).

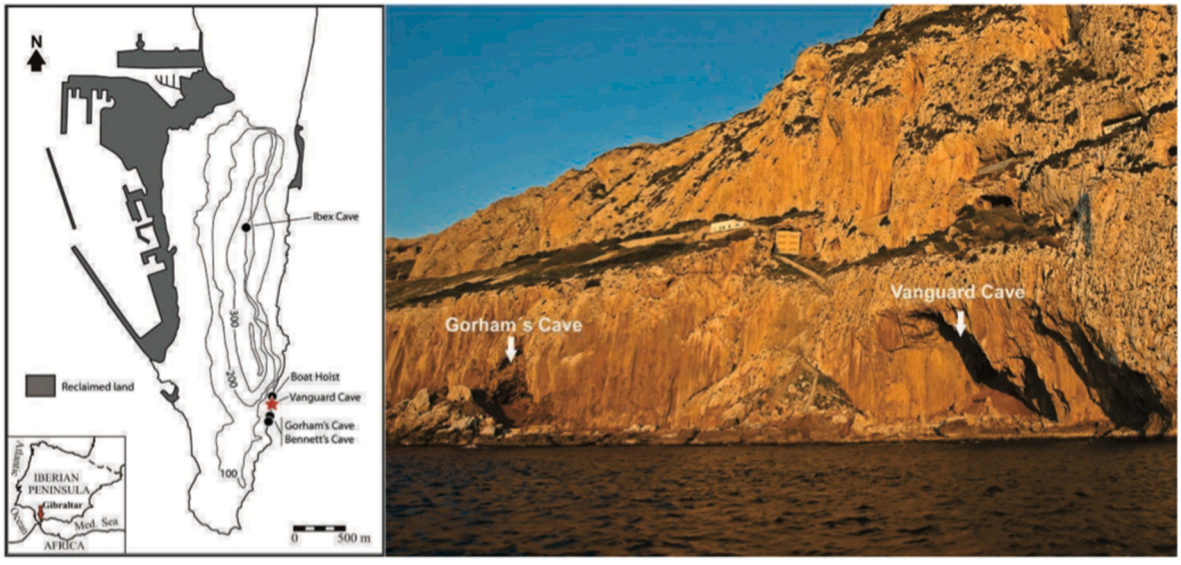

Fig. 1. Location of Vanguard cave in southern Iberian Peninsula.

The sequence exposed in recent excavations (2012-present) contains 25 stratigraphic layers and the chronological control is constrained by 15 OSL absolute age data points (see Doerschner et al., 2019; Table S1). The stratigraphic layers 9–16 (Fig. 2) are similar to the underlying sedimentological layers, characterised by alternating thin (~2 cm) finer grained palaeo-pond deposits with thicker homogeneous sand deposits. Neanderthal presence is indicated by Middle Palaeolithic stone tools in layers 16-14 and 12-9.

The uppermost stratigraphical units at Vanguard Cave, Layers 1–8 are mainly characterised by sands and clays. The faunal assemblage recovered from the uppermost stratigraphic section at VC is dominated by small vertebrates, including rabbits and birds. Many of them were semi-articulated and show no biostratinomic modifications, which suggests that they entered the cave voluntarily. Investigations of hyaena coprolites and bones preserved within the sediments (especially Layer 5) reaffirm that hominids and carnivores alternated in the occupation of the cave. The vertical position of the uppermost layers close to the cave ceiling suggests a low entrance that gradually became smaller as the cave rapidly filled in with sediment. The sand Layers 24, 22 and 18 were subdivided into several sublayers to account for their slightly varying clay contents. Shell fragments and micro-charcoals are present in Layers 19 and 18a, respectively. The exposed layer 25 corresponds with a layer in Area B described by Macphail et al. (2013) as a pinkish-grey ashy deposit resting on more consolidated silty sands with the presence of a hearth associated with a scatter of burnt marine shells and knapping debris, which was interpreted as result of the processing of marine resources by the Neanderthals (Stringer et al., 2008).

Layer 9 was divisible into six subunits (See Supplementary Information. Stratigraphy and Archaeozoology. Layer 9a was characterised by shale and sands (7.5YR/3 brown) of 10 cm maximum thickness; Layer 9b: shale, clay and sand (10 YR 3/3 dark brown), 5 cm thickness; Layer 9c: shale and sands with micro-charcoals (10 YR 2/2 very dark brown), 10 cm thickness; Layer 9d: red shale and sands (10 YR 4/4 dark yellowish brown), 10 cm max. thickness; Layer 9e: sand (10 YR 5/8 yellowish brown); 9g: pit dig mark; Layer 9f: red shale with high sand component (10 YR 4/5 dark yellowish brown), not excavated

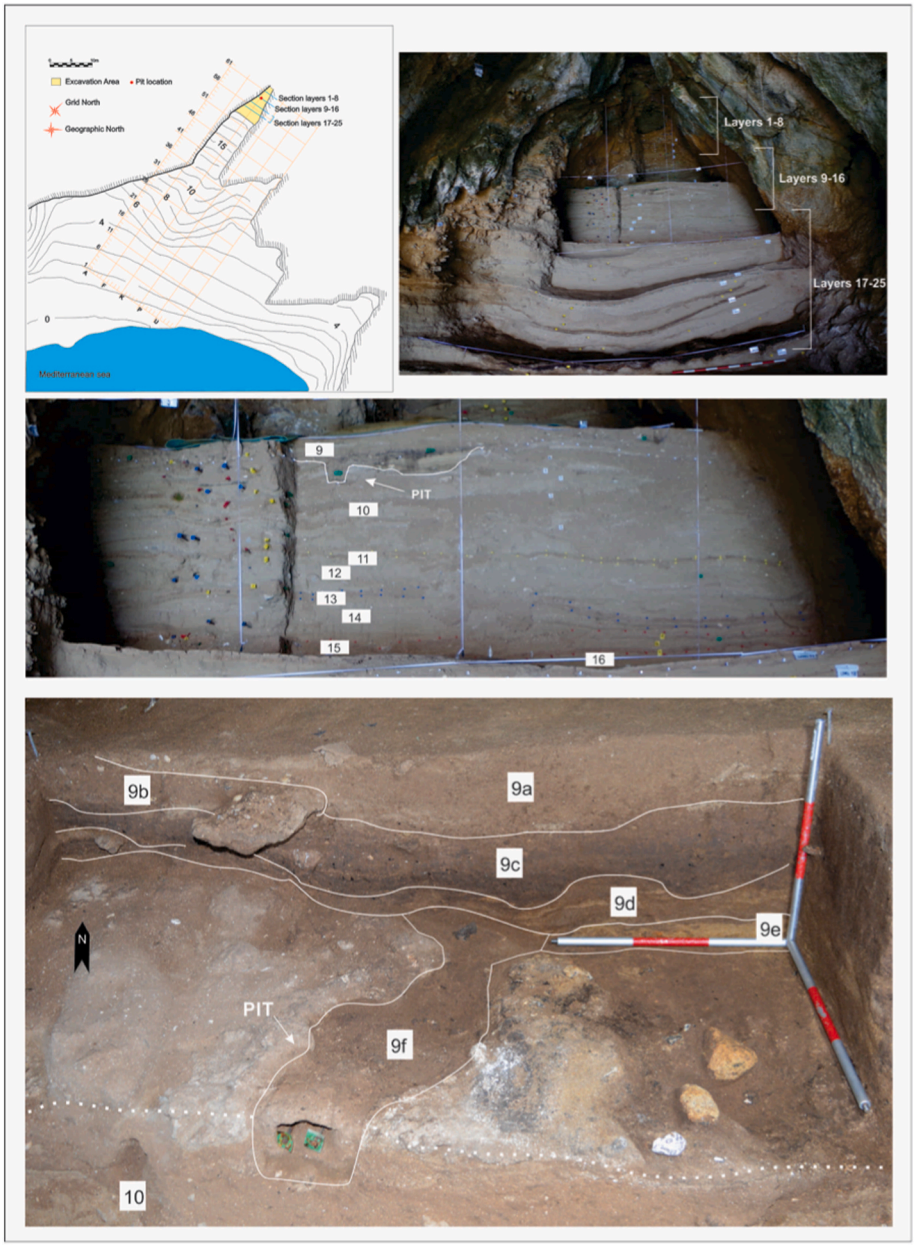

Fig. 2. Plan view map of Vanguard Cave site and pictures showing the section profiles excavated and the section of the pit.

completely. The stratigraphy ends in the layer 10 (surface), characterized by carbonate sands with clear marks of thermo-alteration.

The archaeozoological record in the excavated 3 m^2 of layer 9 (it has a thickness that ranges between 10 cm minimum and 35 cm maximum) is poor with the presence of 96 bones, mostly birds and rabbits, 4 marine shells and 2 microdebitage. This suggests a very short or occasional human presence.

2.3. Chronology

Pettitt and Bailey (2000) analysed seven radiocarbon samples from VC and concluded that the deposits were either close to, or beyond the limits of this dating method. The layers of this VC section (1-24) were dated, recently, by OSL dating in sand-sized quartz grains (Doerschner et al., 2019), using single-grain and multiple-grain dating to clarify the depositional history of the sedimentary sequence. The results suggested that VC experienced relatively rapid and continuous sediment accumulation, probably since the last sea-level high stand in MIS 5 (112 ± 10 ka), and was completely filled by MIS 3 (~43 ka). The presence of the structure was identified in layer 9 and a dug into 10. This hearth has not been directly dated but it occurs between several dated samples that chronologically place it from 67.6 ± 5.3 ka to 60.8 ± 11.0 ka (MIS 4 or early MIS 3) with associated Middle Palaeolithic stone artefacts (Table S1).

3. Materials and methods

The excavation of the layers that covered the pit was carried out following natural layers, based on sediment composition, texture and colour, generating a detailed stratigraphy (Figs. 1 and 2).

3.1. Ichnology

To assess the attribution (or not) of the structure studied as a possible warren, ichnological criteria have been applied. In this sense, its morphological features (possible ichnotaxobases) and sedimentary fill have been analysed. For this purpose, we followed the specific ichnological bibliography (Allen, 1997; Bertling et al., 2007; Milàn and Bromley, 2006; Buatois and Mángano, 2011; Pelletier et al., 2016, 2017).

3.2. Organic geochemistry

The solvents used in the analyses were hexane (HEX), dichloromethane (DCM), methanol (MeOH), toluene (TOL), and acetone (ACN), provided by Merck (GC SupraSolv; 2.5L). All the material was glass, and only in some specific steps of the levoglucosan (LEV) were polypropylene test tubes and microvials used. Centrifuge tubes were 16 × 100mM (10 mL; PYREX), test tubes 16 × 100mM (Corning), pasteur pipettes 150 mM, conical-shaped microvials 1.1 mL (Thermo, Chromacol 8SC; Waters), microvials 1.5 mL amber standards and solvents (Agilent) and 7 mL amber standards preparation vials (Supelco). For the high recovery conical and amber microvials, 8 × 1.5 mM silicone/red PTFE septa (Teknokroma) were used, which were left in DCM and dried before use. All the material that could not be muffled (400 °C; 8h) was washed in ultrasound with 5% alkaline detergent (Extran AP13, Merck), rinsed with distilled water, finally milli Q water, ACN and dried in the oven (40 °C). Small routinely used instrumentation includes ultrasound (Selecta), rotary evaporator, 20 mL tube (Turbovap) and microvial evaporators (SpeedVac SPD120), N2 stream evaporator with thermostat (reacti-vap27POS, Thermo) and centrifuge (Thermo, 5702). Sediment cave samples were analysed by different methodologies that we will refer to as IDAEA and ICTA.

3.2.1. IDAEA protocol for lipids and sugars by GC-MS

As a first step, an exploratory GC-MS procedure was applied by IDAEA to analyze organic compounds, including levoglucosan (LEV), betulin, betulinic acid, polycyclic aromatic hydrocarbons (PAHs), including retene (Simoneit, 1977), alkanes, and alcohols. Therefore, 20 g of cave sediment (4 samples from the area of archaeological interest: VG9f-28_control, VG9f-23, VG9f-24, VG9f-25) were weighted and placed in to cellulose thimble and spiked with 25 μL surrogate standards levoglucosan-D7 and succinic acid-D4 (2000 ng; Cambridge Isotopic Laboratories, UK), n-C24D50 (60 ng; Cambridge Isotopic Laboratories, UK), anthracene-D10, benz[a]anthrancene-D12, benzo[k] fluoranthene-D12 and benzo[ghi]perylene-D12 (60 ng; Dr. Ehrenstorfer, Germany). Samples were soxhlet extracted for 8 h in a 100 mL mixture of organic solvents (DCM:MeOH 2:1 v/v; Merck, Germany). Extracts were filtered for the removal of particles (0.4 μm micro-glass fibre filters and glass syringe; Sartorius, Germany) and concentrated to 0.5 mL by rotovapory evaporation. For the analysis on GC-MS, 25 μL aliquots of the extract were evaporated to dryness under a gentle N2 stream. Then, 25 μL of N,O-Bis (trimethylsilyl)-trifluoroacetamide with 1 % trimethylchlorosilane (Supelco, USA) and 10 μL of pyridine (Merck, Germany) were added for derivation of acids and sugars to their trimethylsilyl ethers and esters in an oven at 70 °C for 1 h. They were concentrated to 0.5 mL by rotary evaporation. The same process was carried out weighing only 2 g of sample (VG9-12, VG9-13, VG9-14, VG9-15), which in this case allowed direct extraction with solvents and an ultrasound bath and evaporation under a stream of N2.

Final sample extracts were injected in to a Thermo gas-chromatograph (GC) coupled to a mass spectrometer (MS) (Thermo Trace GC Ultra – DSQ II) equipped with a 60 m fused capillary columns (HP5MS 0.25 mm × 0.25 μm film thickness) for the analysis of hydrocarbons and derivatized polar compounds. The oven temperature program started at 60 °C held for 1 min, and then it was heated to 120 °C at 12 °C/min. and to 310 °C at 4 °C/min. where it was held for 10 min. The injector, ion source, quadrupole and transfer line temperatures were 280 °C, 200 °C, 150 °C and 280 °C, respectively. Helium was used as carrier gas at 0.9 mL/s. A MS selective detector was operating in full-scan (m/z 50–650) and electron impact (70 eV) modes.

3.2.2. ICTA protocol for levoglucosan by LC-MS/MS

The analytical details for levoglucosan (LEV) analysis have been detailed elsewhere (Davtian et al., 2023). Briefly, extractable lipids and sugars were recovered using a selective pressurised liquid extraction protocol (ASE350, Dionex, Thermo). Extraction cells (10 mL) were filled consecutively with (a) 3 g of activated silica, (b) 3 g of soil sample, and (C) 50 μL of a 200 ng/mL of 13C6-LEV in MeOH; Cambridge Isotope Laboratories). Lipids were selectively extracted with 1:1 Hexane: Acetone (100 °C, solvent saver program, 2 mL/min, 5 min). This fraction was further used for the IDAEA determination of PAHs. LEV and other polar compounds were recovered with MeOH (100 °C, solvent saver program, 2 mL/min, 19 min) and collected in a separate fraction. The polar fraction was further purified using a ligand-exchange solid-phase extraction (LE-SPE) procedure that selectively separates LEV from other polar compounds (see Wöstehoff et al., 2022). LEV extracts were desalted by percolation through columns loaded with 4 g of AmberLite® MB20 mixed-bed ion-exchange resin.

Levoglucosan was identified and quantified using a LC-ESI-MS/MS system (LC-QQQ, Agilent 6470) set up in multiple ratio monitoring mode and negative ions (MRM, 161 > 101 for LEV, and 167 > 105 for 13C6-LEV). Levoglucosan was separated from other isomers (mannosan and galactosan) using a SeQuant® ZIC-HILIC (150 × 2.1 mm, 3.5 μm particle, Merck) column thermostated at 20 °C with a mobile phase flow rate of 0.275 mL/min. The mobile phase was obtained by in-line mixing MilliQ water (Solvent A) and ACN (Solvent B) with a linear solvent gradient programmed from 5% A to 20% A in 8 min. A post-column addition of 0.1 mL/min of a NH4OH solution was used to enhance the MS/MS signal. Quantitation of LEV was calculated using the peak area ratios between each analyte and the IS (13C6-LEV). Linear calibration curves (weighted for 1/X2) were obtained between 10 and 10000 pg

injected. Both LC-ESI-MS/MS control and data acquisition were performed with MassHunter Chemstation software version 10.0 SR1 (Agilent).

3.2.3. IDAEA protocol for PAHs

3.2.3.1. Extraction and purification methodology of ICTA. Identification and quantification were done by GC (Agilent 7890B) coupled to an Agilent 7000A triple quadrupole GC/MS for selective analysis by an optimized multiple reaction monitoring (MRM) methodology. A 5%-phenyl-methylpolysiloxane column was used (film thickness 0.25 μm; internal diameter 0.25 mm; length 30 m) for compound separation. The temperature program began at 90 °C, maintained for 1 min, then ramped to 120 °C at 12 °C/min and to 320 °C at 4 °C/min, where it was maintained for 10 min. The injector, ion source, quadrupole and transfer line were at 280 °C, 200 °C, 150 °C and 280 °C, respectively. Helium was used as carrier gas at 0.9 mL/s. PAHs were identified by retention time and characteristic ions. Both GC-MS/MS control and data acquisition were performed with MassHunter software version 8.0 (Agilent).

3.2.4. ICTA determination of benzene polycarboxylic acids (BPCA)

Approximately, 300 mg of freeze dried soil samples were placed in a 55 ml MARSXpress (CEM Corp.) vessel and oxidised with 5 ml of 67–69 % HNO3 (trace metal grade, Fisher Scientific, Leicestershire, UK) for 6 h at 160 °C in a MARS 6 microwave (CEM Corp.). Sample digests were diluted with water and filtered with a 15 mm diameter glass-fiber filter. The resulting HNO3-containing solution was evaporated using a MARS6 XpressVap evaporation system (CEM Corp.) during 50 min to a final volume of approximately 1 ml. Polyvalent cations were removed chromatographically using a cation exchange resin (20g of Dowex 50Wx8 in the H+ form, 200–400 mesh, Sigma Aldrich, USA). Extracts were diluted with 9 ml of Milli-Q water and loaded onto the column and. BPCAs were eluted with 60 ml of 40 % MeOH. Purified extracts were concentrated using the MARS6 XpressVap system (CEM Corp.) and redissolved in 0,5 ml of 1 % phosphoric acid (Sigma-Aldrich, ref. W290017) in Milli-Q water (LC phase A) and transferred into a 2 ml glass vial prior to LC-UV analysis.

BPCAs were analysed using a high-performance liquid chromatography (HPLC, Infinity II, Agilent) equipped with a diode array detector. Compounds were separated with an Agilent Poroshell 120 SB-C18 column (3 × 100 mm, 2,7 μm), and eluted using a solvent gradient from 100 % A to 30 % A in 10 min followed by isocratic conditions during 2 min. Solvent A was obtained by diluting 1.1 ml of 85 % phosphoric acid with 0.5 L of Milli-Q water. Solvent B was acetonitrile (HPLC-grade, Merck). BPCAs were detected and quantified by their absorbance at 240 nm. BPCA detection and quantification was performed by comparing their absorbance at 240 nm with standard solutions using an external linear calibration curve with a dynamic range of 0.5–100 μg/ml. A linear curve was adjusted using the minimum squared regression method for instrumental calibration. Thermo Chromeleon 7.2 SR4 software was used for data acquisition and processing.

3.3. Inorganic geochemistry

Major elements were measured in Vanguard Cave samples by means of X-Ray Fluorescence (XRF) using a Wavelength Dispersive Spectrometry (WDXRF) Bruker AXS Pioneer S4 at the Andalusian Earth Science Institute (CSIC-University of Granada, Spain). Samples were measured as pressed pellets prepared by pressing about 5 g of ground bulk sediment into a briquet with boric acid backing. The quality of the analysis was monitored with reference materials showing high precision with 1 sigma 1.0–3.4% on 16 data-sets at the 95% confidence level.

Trace element analysis was performed with an inductively coupled plasma mass spectrometry (ICP-MS; PerkinElmer Sciex Elan 5000). Samples were measured in triplicate through spectrometry using Re and Rh as internal standards. The instrumental error is 2% for elemental concentrations of 50 ppm (Bea, 1996). All analyses were performed at the Instrumentations Center for Scientific Research (CIC), University of Granada, Spain.

3.4. Mineralogical and geochemical studies by X-ray diffraction

Selected 11 samples were homogenised by grinding an agate mortar and packed in sample holders for X-ray diffraction (XRD). For clay mineral analyses, the carbonate fraction was removed using acetic acid starting at a very low acid concentration (0.1 N) up to 1N, depending on the carbonate content of each sample (Fig. S15). After successive washing, the <2-μm fraction was separated by centrifugation. The clay fraction was smeared onto glass slides for XRD. X-ray diffractograms were obtained using a PANALYTICAL X'PERT PRO diffractometer (IACT). Scans were run from 2° to 70° 20 for bulk-sample diffractograms, and from 3° to 30° 20 for untreated clay preparation and glycolated and heated (550 °C) clay-fraction samples.

For geochemical analyses, major elements were measured by X-Ray Fluorescence (XRF) using a Wavelength Dispersive Spectrometry (WDXRF) Bruker AXS Pioneer S4 at the Andalusian Earth Science Institute (CSIC-University of Granada, Spain). Sample powders (c. 1 g) were weighed with di-lithium tetraborate flux, and then the mixture was fused at 1000 °C for 15 min. Precision (% RSD), measured by repeated analyses of reference materials as external standards, was better than 1.5%. Trace elements were measured with an inductively coupled plasma mass spectrometry (PerkinElmer NexION 300d) at the Centre of Scientific Instrumentation of the University of Granada (CIC-UGR, Spain). Dissolutions were obtained after HNO3 1 HF digestion of 0.1000 g of sample powder in a Teflon-lined vessel, evaporation to dryness, and subsequent dissolution in 100 mL of 4 vol% HNO3. Instrument measurements were carried out in triplicate using Rh as internal standard. Precision was better than ±5% for an analyte concentration of 10 ppm.

3.5. Charcoal analysis

Charcoal analysis is based on the anatomical study of ~90 samples from 11 sampling units/subunits that were handpicked by the archaeological team. All the charcoalified material was studied under reflected light microscopy. The small size and bad state of preservation of most of the charcoal has not always allowed the neat fracturation of the samples, hence difficulting the obtention of clear transverse (TS), radial (RLS) and tangential (TLS) oriented observations (Figs. S18–S19; Table S7). The analytic procedures used are reported in Chabal et al. (1999). Anatomical features were observed at different magnifications (x50, x100 and x200) and taxonomic identification was achieved using classical manuals of wood anatomy identification (e.g., Greguss, 1955; Schweingruber, 1990; Vernet et al., 2001) and by comparison with the wood reference collection of the Universidad Politécnica de Madrid.

Furthermore, selected samples were mounted on metal stubs, gold sputter coated (to prevent sample charging) and observed on a JEOL 6400JSM scanning electron microscope (SEM) at the Centro Nacional de Microscopía Electrónica (ICTS-CNME) of the Complutense University of Madrid.

3.6. Palynology

The sampling was conducted following Girard (1975). For the extraction of palynomorphs, the "Classic Chemical Method" was followed (Dimbledy, 1985; Erdtman, 1969), with the modifications proposed by Girard and Renault-Miskovsky (1969). To evaluate the quality of the laboratory processing, we added to each sample three tablets of Lycopodium spores. After being treated at the laboratory, the samples were mounted on slides with the use of liquid paraffin. The palynological identification was made by conventional microscopy (400x and 1000x) using an optical microscope. We also used the palynomorph

reference collection of the Department of Plant Biology of the University of Murcia. The pollen count data was treated with the Tilia Graph 1.7.16 program in order to obtain the pollen diagrams.

The analysis has shown palynomorphs with a fairly good level of preservation allowing reliable taxonomical discrimination and frequencies of indeterminable grains averaging relatively low values (Table S8), thus suggesting that differential corrosion is not seriously affecting the pollen assemblages. The number of palynomorphs extracted ranges between 82.97 and 1116.40 grains/g, and from the coprolites fluctuate between 1311.46 and 2265.35. The number of palynological types varies between 13 and 32, with a total of 62 taxa being recognized. Of the 20 samples studied, 13 were polliniferous (Table S8) with the sole exception of four sediment samples and three coprolites, which lacked pollen. A total of 30655 palynomorphs were identified, 3952 pollen grains and 26703 spores were counted, excluding those not identified. Along with cryptogam spores and non-pollen microfossils, we excluded the pollen grains of Genisteae, Asteroideae, Cichorioideae, Apiaceae, Centaurea montana t., and Boraginaceae from the total pollen sum because it is likely they are overrepresented by local abundance. The percentage of indeterminable types remained, in most cases, in values lower than 7% (Table S8). The pollen and non-pollen palynomorphs counts were carried out until reaching a Pollen Base Sum (total of pollen grains, excluding the spores and non-pollen microfossils) of at least 200 pollen grains, except in the two cases in which the reading of all the available material did not allow it (samples VG-3 and VAN'13c2).

3.7. Micromorphology

We used optical and electronic microscopy in order to complete microestratigraphic and micromorphological analysis. Detailed photographs of the deposits have been analysed at mm to cm scale and interpreted and allowed us to select samples for subsequent work in the laboratory. Optical studies allowed us to identify urea and/or resin crystals (Figs. S27–S28 and Figs. S32–S33) and pollen grains.

Bulk samples from individual stratigraphic units were also observed under the scanning electron microscope (SEM) using an AURIGA FIB-FESEM Carl Zeiss SMT microscope equipped with an energy dispersive X-ray (EDX) detector system (Centre for Scientific Instrumentation, University of Granada) and on a JEOL 6400JSM at the Centro Nacional de Microscopía Electrónica (ICTS-CNME) of the Complutense University of Madrid. Electronic microscopy allowed us to identify micromorphological features as the presence of rounded quartz grain morphologies and Ca-phosphate crust (Figs. S16 and S17).

3.8. Microarchaeological analyses (phytoliths, non-siliceous microremains and FTIR)

Twelve Samples were analysed for FTIR, phytoliths and other non-siliceous microremains (Fig. 3 and Table S5). All samples were taken from layer 9 to where the structure belongs. Of these, six corresponded to layers 9a-9f and four to subunits 9f1-9f4 (Table S5). Two control samples were also analysed for comparison. In addition, two more samples were studied corresponding to the tar experiment. Samples were processed and analysed at the Laboratory of the Department of Prehistory of the Autonomous University of Barcelona (UAB).

3.8.1. Phytoliths

Prior to extraction, samples were sieved at 125 μm to remove large particles (mostly quartz). Phytolith extractions were carried out according to (Katz et al., 2010). Between 2 and 50 mg of dry sediment was placed in a 0.5 ml tube. Then 50 μl of HCLN6 was added to dissolve the carbonates. At the end of the reaction, 450 μl of sodium polytungstate (SPT) solution [$Na_6(H_2W_{12}O_{40})\bullet H_2O$] with a density of 2.4 g/ml was added. The tube was vortexed and sonicated for 10 min and then centrifuged at 5000 rpm for 5 min 50 μl of the aliquot was placed on a microscope slide and covered with a 24 × 24 mm coverslip.

3.8.2. Non-siliceous microremains

After sieving the samples through a 125 μm mesh to remove larger particles (mostly quartz), approximately 1 mg of sample was placed on a microscope slide and 4–5 drops of Entellan (new Merck) were added. Samples were homogenised in the slide and covered with a 24 × 24 mm coverslip. Despite some samples presenting ash pseudomorphs, these were recorded in low numbers and, thus, have been recorded as presence/absence in Table S5.

3.8.3. FTIR

Samples were also analysed using Fourier Transform Infrared (FTIR) spectroscopy, which provides a quantitative assessment of the mineral composition of sediments. In a first step, the samples were analysed by FTIR prior to sieving to observe the gross mineralogical composition. In a second stage, the samples were sieved on a 125-μm mesh and analysed again by FTIR to better observe those minerals that may have been masked by the presence of quartz, which was clearly present in the samples. The methods used follow those of (Weiner, 2010). Tens of micrograms of sediment were homogenised with KBr to obtain the pellets. Infrared spectra were obtained in transmission mode using a

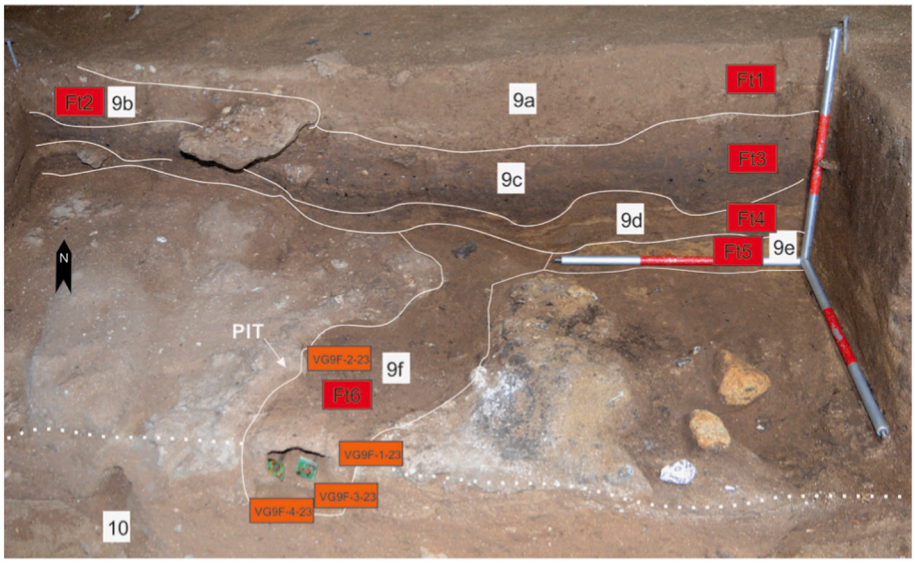

Fig. 3. Location of the phytoliths (Ft) samples (red rectangles) and associate archaeological layers.

Nicolet iS5 spectrometer at 4 cm-1 resolution and in 32 scans in the 4000-400 cm-1 spectral range. To assess the origin of calcite, when present, we applied the infrared grinding curve method (Regev et al., 2010) based on the measurement of the ν2 and ν4 intensity (874–875 and 712-713 cm-1, respectively) normalised to the ν3 intensity (14291436 cm-1). Normalised intensity values were compared with reference grinding curves published in (Macphail and Goldberg, 2000). Band shifts of clay minerals exposed to elevated temperatures, described in (Berna et al., 2007), were used to determine the possible thermal alteration of clay minerals in the sediments. Additionally, the FTIR reference collection of standard materials provided by the Kimmel Center of Archaeological Science, Weizmann Institute of Science was consulted (http://www.weizmann.ac.il/kimmel-arch/infrared-spectra-library.mel-arch/infrared-spectra-library).

3.9. Experiments developed to analyze the potentialities of Cistus ladanifer to produce tar based in the structure found in Vanguard Cave (layers 9 and 10)

The goals of the experimental activities carried out were to demonstrate that the use of the structure found in Vanguard Cave, Gibraltar (Layers 9 and 10) for the production of tar (Fig. 1), as well as to understand in a functional way its morphology and composition in the context of an operative process. We start from the initial hypothesis presented in the discussion of our manuscript and seek to use technologies recognized for Neanderthals to understand whether it would be possible to produce tar from *Cistus ladanifer*, whose present evidence of this Mediterranean species is widely discussed in our work.

It is relevant for the present study to prove that is possible to produce significant amounts of tar from rockrose (*Cistus ladanifer*) brown resin, called labdanum, using only materials and techniques that would be available to Neanderthals in the surroundings of Vanguard Cave.

For the purposes presented, four archaeological experiments were performed in the open air in a private farm in Portelas (Alvega, Portugal), with a structure that sought to be a reproduction of the size, morphology, materials and dimensions of the VC Layer 10 structure (Figs. S24 and S25). The choice for the experimental place was related with the proximity to the raw material (rockrose), growing wild in Mediterranean-like shrubland. The experiments took place in November 2022 and January 2023, at the end of a long period of drought when the plants were dry, and after one month of intensive rain, respectively. We could not find significant differences in the weight of young leaves obtained neither the volume of tar produced, for the two periods selected to develop the experiments. The protocol of the experiments was designed following the model interpreted from the evidence in Vanguard Cave.

4. Results

4.1. Ichnology

Several Pleistocene mammal and bird species found in Gibraltar are fossorial animals that produced burrows (as troughs or tunnels) or burrows systems, with the function of either shelter, food foraging, hibernation and nesting (Rodríguez-Vidal et al., 2013). Some of them, like foxes, badgers or crested porcupines are just too large to produce burrows comparable with the size of the structure under analysis. The fossil record of small mammals (rabbit, mole, vole, dormouse and shrew) in Gibraltar should be discussed as potential tracemakers of the structure.

The European rabbit bones are common in the sequence where the structure was found (Doerschner et al., 2019). The *Oryctolagus cuniculus* has a head-body length of 340–500 mm and lives in 3D-complex networks of interconnected (galleries, chambers and turning chambers) permanently open known as warrens excavated by small number of individuals that live in society to ensure greater breeding success (Pelletier et al., 2016). Burrow networks are usually unlined (Pelletier et al., 2017) and show a vertical development (at least on two layers) (Fig. S26). The social structures tend to be looser in areas where burrow construction is relatively easy such as sand dunes, developing separated breeding "stops" lined with belly fur (Fig. S26). Single burrows can even occur in low population densities. Burrows diameter varies between 100 and 500 mm (Kolb, 1985).

The Mediterranean mole has a head-body length of 95–143 mm. It develops a semi-permanent foraging 3D burrow system plus one or more sleeping chambers, shallow to over 10 m deep (Godffrey, 1955), but usually avoids sandy soils because it cannot construct a proper burrow system that can be revisited to collect insects or annelids, due to frequent collapsing. In these sedimentary environments burrows are often simple tunnels (Kolb, 1991). The shrews, voles, mice and moles also build burrow systems but are just too small (head-body length less than 100 mm, except for the *Microtus cabrerae* (up to 140 mm) and the water vole, but this burrows in close proximity to a lake or river) to produce burrows and chambers with the size of the structure under analysis. The hare *Lepus temidus* rarely burrows, preferring to occupy others burrows. Head-body length varies between 457 and 610 mm. Sometimes it digs burrows as shelters for leverets. Finally the garden dormouse develops winter hibernation burrows but its habitat is confined to thick-shrub layer woodlands. These burrows are oval shaped, 180–700 mm long and 120–200 mm in the widest part (Jurczyszyn, 2007).

4.2. Organic and inorganic geochemistry

Organic compounds, such as n-alkanes, alcohols, urea (2TMS), and citric acid (4TMS) were identified by the retention time and the characteristic m/z fragments (Figs. S1 and S2). The applied GC-MS methodology was not sentitive enough to detect LEV, betulin, betulic acid, and PAHs well above blank or control levels. Therefore, more sensitive and selective extraction and detection procedures were applied by ICTA and IDAEA using 5 g of cave sediment (4 samples from the area of archaeological interest: VG9f-1_23, VG9f-2_23, VG9f-3_23, VG9f-4_23) (Figs. S2–S14).

Levoglucosan (LEV) and retene was detected but not mannosan (MAN) nor galactosan (GAL) (See Tables S2, S3 and S14). Levoglucosan values ranges from 1 to 16 ng/g, with the highest values in these samples associated to the core of the structure (VG9-13 and VG9-14). Obtained results for Benzene Polycarboxylic Acids (BPCA) in 5 samples inside the structure (Table S4) indicate a ratio B5CA/B6CA uniform and thus the samples analysed belong the same black carbon type of composition (ca. 0.7–1). These values are consistent with ratios obtained in Pleistocene archaeological samples in the Mediterranean Sodmein Cave (Wöstehoff et al., 2022). Retene was found in concentrations from 1 to 4 pg/g in all VG9f-23 samples (Fig. 4)

A total of eight samples were measured along VC Layer 9. Cu content varies from 9 to 186 ppm and Zn from 38 to 290 ppm at Layer 9 (Table S6), with lowest values in both cases in these samples distanced from the structure.

4.3. Charcoal analysis

The charcoal specimens that have been studied frequently crumbled and disintegrated. They were extremely fragile and many samples were compressed. Only a small number of samples have been recovered in a state of preservation sufficient for identification. Decay caused the wood to lose part of the cell wall components and to compensate the loss with water imbibition. As a result, the recovered samples had poor mechanical properties, and were extremely perishable especially by drying at room temperature.

Exceptionally (9B-II), some specimens of Cistaceae have been found partially vitrified, a state at which the different anatomical elements of the wood appear to be fused (Fig. S18). Also, some of the samples were incompletely burned, as part of the specimen were not charred.

Another distinctive feature of the charcoal assemblage is the high

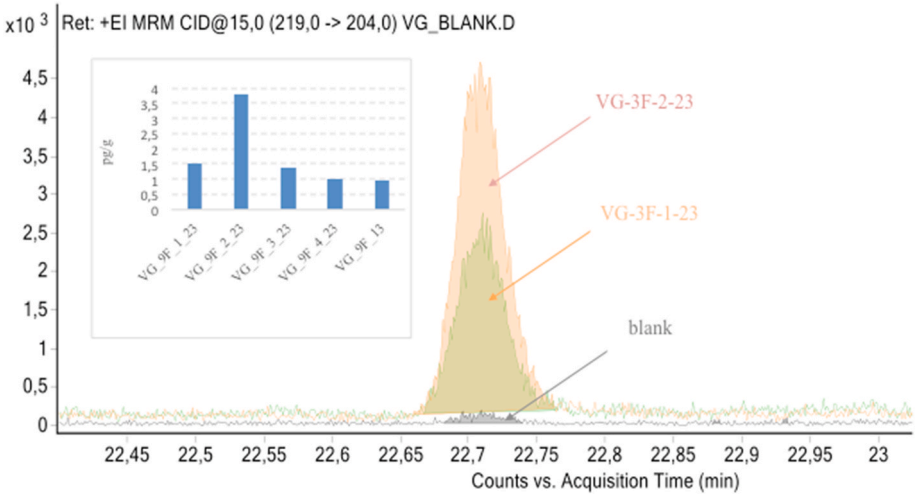

Fig. 4. Gas chromatograms and Multiple Reaction Monitoring signals and concentrations of retene detected in samples of the archaeological structure and blank (see details in the Supplementary Information).

frequency of low-diameter (<2 mm) angiosperm twigs, especially in 9AII and 9EII (Table S7). In these samples, only pith and primary growth are observed, thus preventing accurate wood identification. Other unidentified charcoal remains do not present a wood anatomical structure and might correspond to barks, scales, calluses or undetermined lignified vegetal organs.

Table S7 shows the taxa that are present in the assemblage. It must be noted that conifers (i.e. *Pinus*, Cupressaceae) were more easily identified than other taxa, due to their clear and unequivocal woody features (i.e. homoxylous wood and cross-field pits) (e.g., Greguss, 1955; Schweingruber, 1990; Vernet et al., 2001) (Fig. S19). However, they are poorly represented in the charcoal assemblage, accounting for less than 10% of the total.

4.4. Palynology

Previous palynological analyses in the site were based on coprolites (Carrión et al., 2018), which complemented the work in Gorham's Cave (Carrión et al., 2008). Here we show the results of the pollen analysis of both sediment and new coprolites (Table S8).

Although the pollen samples exhibit particular differences in the presence and abundance of specific taxa, both the sediment and coprolite samples show a similar floristic assemblage, with out of 30 taxa shared by both kinds of samples. The sediment samples show the dominance of *Artemisia* and evergreen *Quercus* (Fig. 5 Part 1-Part 2, S20). Other pollen taxa may reach relatively high values, such as *Pinus* t. (includes *Pinus halepensis-pinea* t., *P. nigra-sylvestris* t.) (VG-3, 6, 4B and VG-1-Layer 10), *Juniperus* (VG-6, 4B, VG-1-Layer 10), *Olea* (VG-4A, 4B, VG-1-Layer 10), Ericaceae (VG-1, 3, VG-1-Layer 10), Poaceae (VG-6), and Amaranthaceae (VG-4A) (Fig. 5 Part 1-Part 2, S20). The coprolite samples show *Pinus*, *Juniperus*, evergreen *Quercus*, Ericaceae, *Artemisia* and Poaceae as pollen dominants.

The palaeoecological context of the findings is outstanding taking into account the pollen deposition that took place in a full-glacial stage. A high diversity of trees, shrubs, and herbs has been found abundantly in both sediment and coprolite pollen samples. Broad-leaved trees include deciduous *Quercus*, *Quercus suber*, *Alnus*, *Betula*, *Corylus*, *Fraxinus*, *Populus*, *Salix*, *Castanea*, and *Juglans*. Mediterranean woody shrubs and trees include *Pistacia*, *Buxus*, *Phillyrea*, *Ceratonia* and *Rhamnus*. Among the conifers, we have identified *Pinus pinaster* and *Taxus*. Xerothermophytes include *Maytenus*, *Calicotome*, and *Myrtus*. Indicators of saline substrates (mainly Amaranthaceae), and heliophytes such as Asteroideae, Cistaceae (VG-1, 5, and VAN'13c3), and *Ephedra fragilis* (VG-1, 3, and VAN'13c1), are also present. In lower frequencies but still common, are Genisteae, Caryophyllaceae, Urticaceae, *Plantago*, Liliaceae, Lamiaceae, and *Centaurea*. Altogether this suggests the local existence of a biodiversity hotspot with several vegetation belts represented in the pollen spectra of two different pollen sources. Non-pollen palynomorphs include mainly pteridophyte spores (monolete and trilete), *Diporisporites*, *Glomus*, *Inapertisporites*, *Microsporonites*, and *Monoporisporites* (Fig. S20), suggesting organic matter decomposition in forested environments.

Previous palaeobotanical studies of Vanguard Cave (Carrión et al., 2018), within the western Mediterranean context, showed the extraordinary disposition of the southern coasts of the Iberian Peninsula to host the most thermic refugium of the Late Quaternary. This pollen analysis on hyaena coprolites (Layers 4–6) shows *Pinus*, Poaceae, Chenopodiaceae, and evergreen and deciduous *Quercus* accompanied by *Alnus*, *Betula*, *Castanea sativa*, *Corylus avellana*, *Juglans regia*, *Fraxinus*, *Salix*, *Ulmus*, *Olea europaea*, *Phillyrea*, *Buxus*, *Coriaria*, *Myrica*, *Rhamnus*, and significantly, the thermophytes *Maytenus senegalensis*, *Withania frutescens*, *Calicotome*, *Pistacia lentiscus*, and *Myrtus communis*.

The new pollen record of VC (Layers 9 and 10) indicates that the site was surrounded by shrubby grassland, savannahs, temperate trees, Mediterranean scrub and Ibero-Maghrehian thermophytic formations. The pollen-bearing coprolites and sediment of Vanguard Cave show several pollen dominants: *Pinus*, *Artemisia*, Poaceae, *Quercus*, *Juniperus*, *Olea*, Cistaceae and Ericaceae. The thermophilic character of the coastal communities is confirmed by the pollen occurrences of *Maytenus*, *Calicotome*, *Ephedra fragilis*, *Myrtus*, *Pistacia*, *Olea*, *Phillyrea* and *Asphodelus*.

4.5. Microarchaeological analyses

The FTIR results in layers 9a-9f distinguish two distinct groups, samples from layers 9a-9c, characterised by a higher presence of clay and quartz (major clay band at 1036-1033 and major quartz band at 1079-1077), the presence of carbonates from calcite, in particular the sample from layer 9a (band 1429), and phosphates (bands 603, 563) (Figs. S29a and b). The second group (samples from Layers 9d to 9f) was dominated by quartz, especially Layer 9e, and clay to a lesser extent, and the absence of carbonates. Phosphates were presented on a lower level (Figs. S29a and b).

4.5.1. Samples 9f1-9f4

All the samples from subunits 9f1 to 9f4 were dominated by clay minerals, although quartz was more abundant in 9f3 and 9f4 (Figs. S30a and b). In addition, all samples contained carbonates from calcite, although to a lesser extent in subunit 9f2 where the presence of

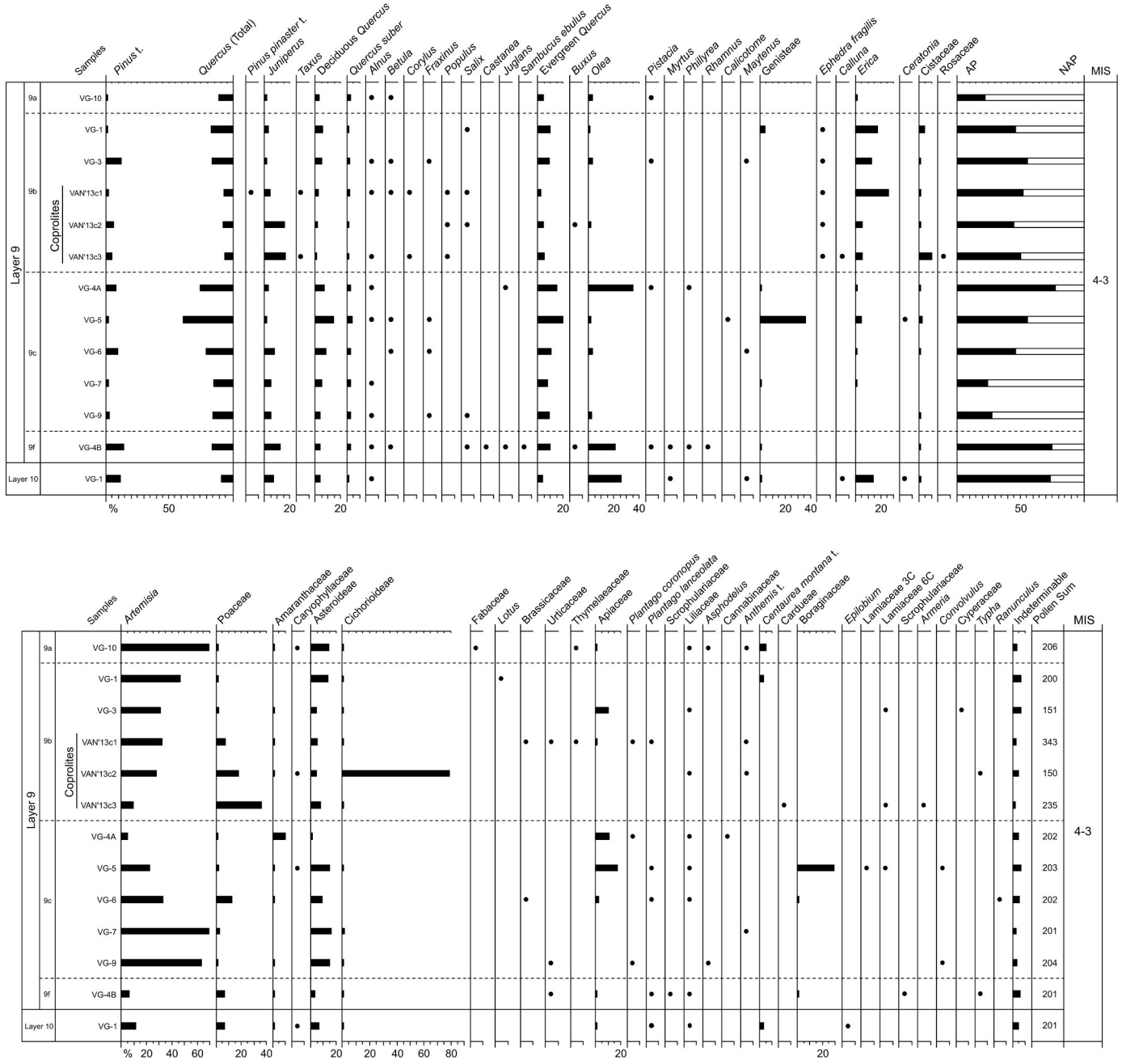

Fig. 5. Pollen diagrams from Vanguard Cave (Layers 9 and 10). **Part 1.** Percentage pollen diagram of the woody component. **Part 2.** Percentage pollen diagram of the non-arboreal elements. Sediment samples (Layer 9: VG-10, VG-1, VG-3, VG-4A, VG-5, VG-6, VG-7, VG-9, VG-4B; Layer 10: VG-1) and coprolites (Layer 9: VAN'13c1, VAN'13c2, VAN'13c3). Genisteae, Asteroideae, Cichorioideae, Apiaceae, Boraginaceae, and *Centaurea montana* type are out from the total pollen sum. Black dots for percentages below 3%. Dashed lines for subdivisions within archaeological layers.

phosphate minerals was higher. The presence of phosphates in all samples is clearly shown in the samples sieved after the removal of large quartz particles >125 μm (bands 603 and 563) (Fig. S30b). As indicated by the presence of clay structure water (bands 3689 and 3619) and bands 915 and 515 in all samples, there was no evidence of thermal alteration of clay >500°(*57*) (Figs. S30a and b).

4.5.2. Siliceous and non-siliceous microremains

Samples were analysed under the petrographic microscope to identify microremains at 400x. Consistent with the FTIR results, clay and quartz were abundant in the samples. In contrast, siliceous microremains such as phytoliths and diatoms were rarely identified. Only few phytoliths were identified in subunit 9f3, but in very low amounts, and one probably melted phytolith was noted in 9f2. Other non-siliceous microremains included the presence of ash pseudomorphs although in very low numbers (Table S5). Ash pseudomorphs are the result of the combustion of calcium oxalate crystals, which grow mostly in dicotyledonous plants. Associated with the ash pseudomorphs, microcharcoal fragments were also recorded in most of the samples. We also observed some irregular isotropic morphologies with a yellowish colour.

4.5.3. Experimental tar samples

The FTIR results of the two experimental tar samples were practically identical (Fig. S31). These tar samples were also analysed microscopically at 400x. Both samples were dominated by irregular isotropic morphotypes with a bright yellow colour similar to those observed

under the microscope at Layer 9, albeit in small numbers and interpret as uric acid or resin (Figs. S32 and S33).

5. Discussion

5.1. The structure: anthropic or biological origin

The structure is a circular trench with a 20–26 cm E-W diameter and 22 cm N-S. This circular trench serves as the axis from which two conduits start: one has a north direction 13 cm long and 9 cm wide; the other has a southerly direction and is 7 cm long, with a morphology of inclined straight walls with a surface width of 12.5 cm and a depth of 9 cm at the bottom where it acquires a base with "two-lobed" shape. The excavated pit had a depth of 9 cm in the circular area, with vertical walls, and 8 cm in the areas with channel morphology (Fig. 2; Figs. S21–S25). The gravitational infilling of this structure is indicated by the downward bending of overlying sedimentary lamina. The structure shows an irregularly thick wall lining, in the bottom and vertical walls, composed of darker (eventually more cohesive) material than the structure filling. The wider side of the structure seems to end close to the vertical wall of the excavation. In both sides of the wider area of the structure there is a splay of fine sediment, sediment flakes and rock fragments developing marginal rims and showing certain metamorphism by high temperatures that provides more consistency to sediments that would otherwise be non-cohesive. The marginal rim resulted from accumulation of sediments in the periphery of the structure by digging action.

Interpretation as burrowing by rabbits or other small mammals over layer 10 would lead us to expect, associated to the burrow wall, marginal micro-folding (around) and high-angle micro-faulting (under the imprint) in the layered sequence associated with a ductile and brittle behaviour of the sediments, respectively, as seen in the experimental mammalian tracks models of Allen (1997). In the structure under study we find, instead, clear-cut walls without evidence of vertically directed deformation of the layers (Fig. 3). This demonstrates that the structure was made as a horizontally open hollow. These layers became firm enough to prevent the vertical-walls from collapsing after excavation or use of the structure, allowing the next sedimentary event to fill it (sublayer 9f).

Detailed ichnological analysis it allows to establish.

i) The preservation of the structure as a semi-relief with passive filling by the downward bending of the overlying bed lamina is evidence against post-depositional burrowing by fossil mammals or nesting birds;
ii) The burrows of these animals usually consist of tunnels and blind chambers. Although they can collapse, there is no evidence of such processes in the studied structure;
iii) The dimensions of the structure are compatible with those of bioturbation structures produced by small mammals (i.e. rabbits, shrews, voles, mice and moles). However, their excavating behaviours commonly result in more complex burrows or warrens;
iv) The presence of a sedimentary lining acts against any burrow chamber since mammals usually line their burrow chambers with grass, moss, leaves and other dried vegetation, feathers or fur, not secreting any binding material or building any wall structures;
v) The marginal rims of expelled sediments away from the structure in low-angle over-thrusted lamina may be evidence for digging activity in any orientation towards the verticality. They were later subject to thermal alteration which resulted in a differential consistency with positive relief (and possibly in the lining visible in the structure walls and bottom);
vi) On the other hand, there is no evidence of loading structures (microfaults and microfolds) at the lower part of the studied structure. This feature fits with the idea that the structure would not correspond to the track of a bigger mammal. In contrast, such loading structures used to be very common and easily recognizable (as occur in the overlying layer).

In summary, the ichnological analysis performed rejects a biological origin for this structure, as either a track or a burrow.

5.2. Structure reconstruction

The excavated structure presented a more complex morphology than that of a simple basin, resembling a pit with a broader central area and an almost squared cross section in the anterior-most part which had been cut by the excavations (Fig. 2, S24 and S25). Lipid compounds were analysed in solvent-extractable fractions from samples from inside and outside the structure. In all samples we observed abundant, straight-chain (i.e., normal, *n*-) alkanes (C27 to C33) (Figs. S2–S12). These are lipid components of the protective waxes that coat the leaf surfaces of almost all land plants and they are mixtures of long-chain *n*-alkanes and alkanols (Eglinton and Eglinton, 2008; Kohn, 2010). The samples present a strong odd-numbered predominance (carbon-number preference index, CPI >9), and C31 as the most abundant alkane. We also observed an abundance of C24-C32 *n*-alkanols with strong even-numbered predominance (CPI >8), and C28 as the most abundant homologue (Table S2, Fig. S4). Given that *n*-alkanes are predominately of odd carbon number and the *n*-alkanols are of even carbon number, the biomarkers in the samples are highly conserved as fresh leaf wax. We also analysed the extracts for levoglucosan, retene, betulin, and betulinic acid. We selected these compounds because they are associated with combustion (Medeiros and Simoneit, 2007) and tar used by Neanderthals (Schmidt et al., 2019; Kozowyk et al., 2023). Levoglucosan, betuline and betulinic acid were in the limit of quantification with the GC-MS method (<20 ng/g) as well as with the more sensitive LC-MS/MS method (<0.1 ng/g) (Figs. S13–S14; Table S3), though retene was found in concentrations from 1 to 4 pg/g in all VG9f-23 samples (Fig. 3). Detection of retene, a polycyclic aromatic hydrocarbon is typically associated with resinous plant combustion or *in situ* generation after degradation of diterpenoid acids, such as abietic acid, in conifer resin and other high plant lipids. We analysed benzene polycarboxylic acids (BPCAs) (Table S4) to further investigate the existence of pyrogenic carbon in a number of horizons and significant concentrations of BPCAs were detected in VC layer 9f (0.008–0.018%). For comparison, char samples from the combustion experiments (Suplementary Information 2) produced 2.3% of BPCAs. Accordingly, BPCA analysis confirmed the abundance of pyrogenic materials in all analysed layers. The relatively uniform B5CA/B6CA ratio (ca. 0.7–1) indicates a similar degree of pyrolysis for all samples, suggesting that they were originated from similar thermal/pyrolytic processes.

The sediment samples from the structure are mainly composed of quartz and feldspars, and variable amounts of calcite and clay minerals. Variations in the content of these latter minerals are remarkable and samples within the structure contain a low content of calcite while those from outside contain abundant calcite (Fig. S15). The samples from outside the structure were also very poor or barren in clay minerals. Clay mineral assemblages were mainly composed of illite and chlorite. Selected SEM images, FTIR and EDX analysis (Figs. S16–S17) confirm the presence of phosphates in some samples and abundant rounded quartz sand grains, which are typically associated with sand dunes, as those surrounding and infilling Vanguard Cave. Microarcheological analysis indicates that phytoliths and other siliceous microremains are not preserved, but instead, microcharcoal fragments, few yellowish crystals (likely tar), and a few ash pseudomorphs from burned woody plants were noted (Table S5).

Significant differences in trace and major element contents were also found. In particular, the content of Zn and Cu in samples infilling the structure was double, or more than triple in some cases, that from outside the structure (Table S6). The results obtained are coherent with a previous study from Gorham's and Vanguard Caves that demonstrate a

link between Zn and Cu enrichments and the presence of burnt guano and/or ash deposits (Monge et al., 2015). The FTIR results indicate that analysed clay minerals within the structure show no evidence of clay heating >500 °C, which can be interpreted by the structure void infilling by a mix of *in situ* (combusted) and lateral (unaltered) sediments. Furthermore, the presence of phosphates in samples is consistent with guano presence.

Only a small number of charcoal samples have been recovered in a state of preservation sufficient for identification. Exceptionally, some specimens of Cistaceae have been found partially vitrified, a state at which the different anatomical elements of the wood appear to be fused (Fig. S18). Also, some of the samples were incompletely burnt, as part of the specimens were not charred. Another distinctive feature of the charcoal assemblage is the high frequency of low-diameter (<2 mm) angiosperm twigs (Table S7). Table S7 shows the taxa that are present in the assemblage. Even though conifers (i.e. *Pinus*, Cupressaceae) were more easily identified than other taxa (Fig. S19), they were poorly represented in the charcoal assemblage, accounting for <10% of the total. It is also noteworthy that, while most detritic-rich sediment in Vanguard Cave is palynologically sterile, the structure itself was rich in pollen grains together with spores of coprophilous fungi, which suggests preservational sealing such as observed in burnt cow dung (Carrión et al., 2000). In addition, pollen spectra are similar to those in coprolites in the same stratum, which precludes the possibility of pollen reworking or contamination (Fig. 5 Part 1-Part 2, S20; Table S8).

The structure studied embraced parts of layers 9 and 10 of the cave sequence. When these layers were exposed, the cave was almost filled with sediments and the distance from layer 10 to the cave ceiling was just 2.5 m (Figs. S21–S25). The structure is located at the deepest and most central position in VC, a place with good illumination from the entrance and sheltered from the commonly-windy Gibraltar environment. Profile A-A' shows that the structure has an open kneading trough profile, unique in the entire cave sequence, and is clearly different from a V-shape water trough (Figs. S21–S25) or animal-made elliptical burrow sections (Fig. S26). Detailed ichnological analysis discarded a non-anthropic origin for this structure. Taking into account the almost general absence of pollen in the sedimentary sections of VC, the occurrence of pollen in the structure studied here also suggests an anthropogenic origin (Dimbledy, 1985). Bioturbation by animals would have oxygenated the sedimentary environment and destroyed any pollen (Carrión et al., 2009). In addition, we did not find any mixture of recent and reworked pollen, typical of recently bioturbated deposits (Carrión et al., 1999). The anthropogenic structure described here could have been shaped through a series of steps that indicate the complexity of the structure and of the thought processes required to plan and execute it (Fig. 6).

5.3. *Proposed sequence of processes involved in the preparation of the structure (Fig. 6)*

- T-0 and T-1: Layer 10 excavation and acquisition of channelled and round kneading through empty space. Bends at layer 9c are supported with the excavation by hand or using a flat wood tool of one person facing the entrance. The placement of carbonate rocks in the channels or the structure as can be observed in Fig. 6 are likely to have stabilised the cover.

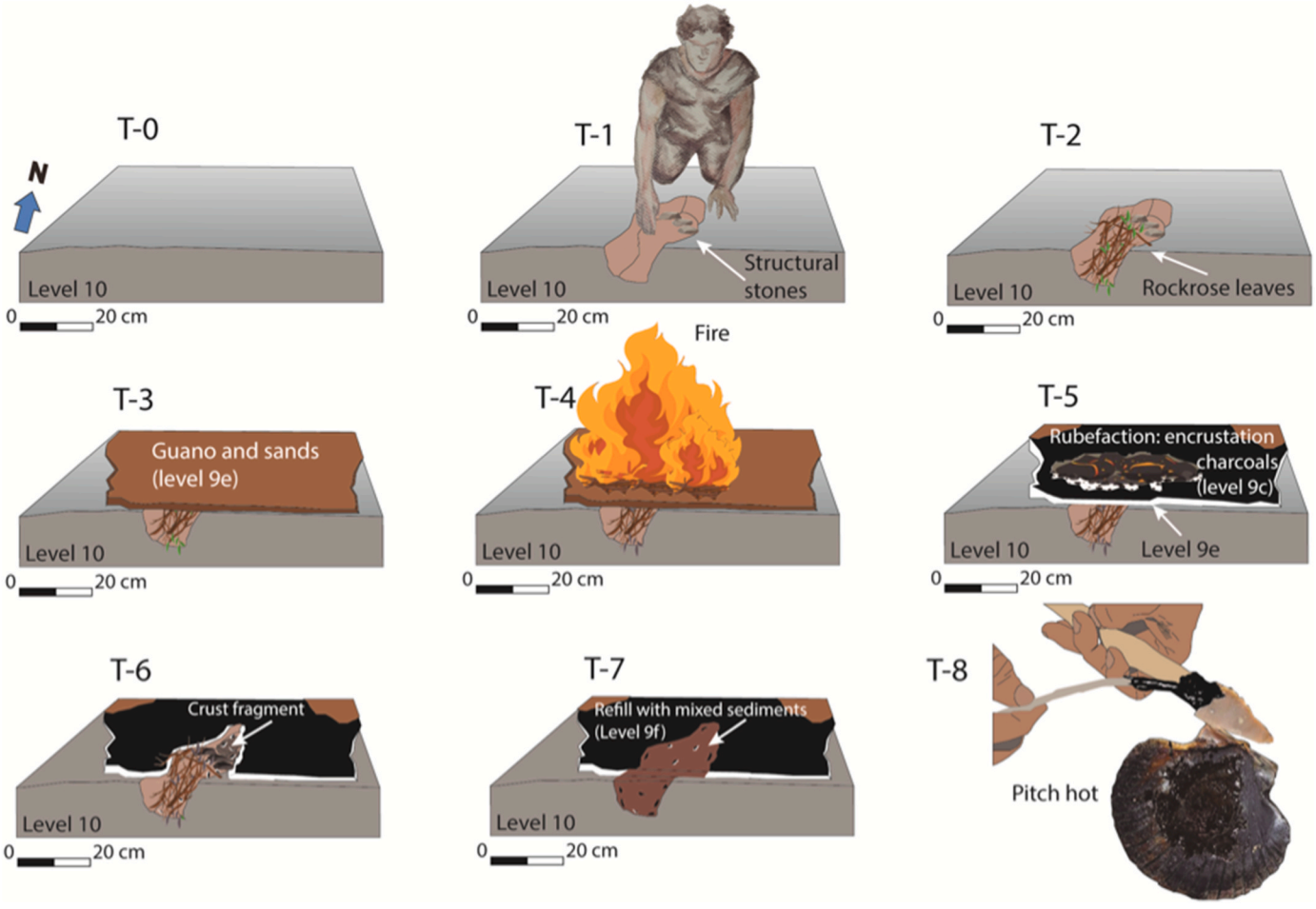

Fig. 6. The anthropogenic structure could have been made following these steps. From T-0 to T-8. Details of each step in the main text and Supplementary Information.

- T-2: Rockrose leaves introduced in the trough, then heated. Thereafter, the trough would be sealed, thus preventing oxidation.
- T-3: A layer of guano is added to the underlying sand to give consistency to the structure and perhaps improve thermal/oxygene insulation.
- T-4: A fire is performed over the trough affecting the contents including the guano layer. Hearth location at the bottom of an almost infilled cave will allow to control wind and therefore oxygen input and temperatures that will be reached. Both sand and guano will allow temperature control.
- T-5: After combustion, the guano would have been rubefied and could have originated the hard crust with the white spherules.
- T-6: Excavation and likely recovery of the material placed in the trough (rockrose resin). This rubefacted guano crust appears to be broken in order to access material deposited in the pit.
- T-7: Infilling of the trough by sediments enriched in charcoal. Structure sealing by layer 9f.

5.4. Structure potential function

The fuel used in the structure seems to have been grass (Poaceae) and other herbaceous vegetation, along with shrub taxa (Cupressaceae and *Erica*), according to the palynological, anthracological, anthropological and organic geochemical analyses. There is no occurrence of bones or tools that could have been used for cooking in this structure. The grass fire allows a faster combustion and a lower, more controllable temperature than using only hard woods, which produce embers with a higher calorific value. The appearance of Cistaceae charcoal fragments in a pyrophytic context supports the idea of a controlled burning of plant material within the pit (Burger, 2016). High Zn content, as the ones described in VC layer 10, have been related here and in other caves to the presence of guano (Monge et al., 2015). The presence of urea and citric acids point to the presence of diagenetically-altered guano. Guano is an excellent context for pollen preservation (Marais et al., 2015). Ignition and handling by Neanderthals explains (by sealing, compaction and anoxia) the presence of pollen inside the structure. Yellowish crystals (likely tar) also are present in a few archaeological samples and with experimental archaeology (tar) (Figs. S27–S28 and Figs. S32–S33).

Our structure matches that of a complex one used for birch tar recovery, described by Kozowyk et al. (2017), which would require a reducing environment and a high level of temperature control as pitch/tar is made at controlled temperatures (Koller et al., 2001). Recent studies demonstrate that distilled tar used by Neanderthals was obtained by underground environment that restricted oxygen flow (Schmidt et al., 2023). In our study, organic molecular tracers measured in samples taken from the inside of the pit are not related to high temperatures. The organic material is related to plant tissues, most likely degraded (rotten) plants. The presence of guano and the decomposition of organic matter produce humic substances and organic acids that could contribute to the observed decrease in calcite content in samples associated with the structure (Hoch et al., 2000). Thermal decomposition of calcite starts at 700 °C, in a low pressure environment, and rapidly occurs >750 °C, a range of temperatures that exceed these expected in an open fireplace (Karkanas, 2021) but easily reached during the experiment (Fig. 7). With the pitch still hot and elastic, it can be applied to adhere a spearhead using shells as container, since they are present in Vanguard cave archaeological layers.

The appearance of charcoal fragments taken from the inner part of the pit, identified as remains of species within the Cistaceae in a controlled burning structure, allows us to infer potential uses as the obtention of tar. The pyrophytic character of most of the Cistaceae (Moretti et al., 2006), and their use to obtain resins and their exudates in the pharmacological and aromatic industry are well established (Frazão et al., 2018). In order to confirm this hypothesis we completed a series of experimental activities and checked if an identical structure to the one found in Vanguard Cave could be used as a kiln for the production of tar.

Fig. 7. Experiment 4: The pit structure was built by hand according to the morphology and dimensions defined by the archaeological excavations in Vanguard Cave (Layers 9 and 10). (a) The pit was filled entirely with ~1.9 kg of young leaves. The rockrose bundle was then sealed with a <2 cm thick layer of the same marine sand mixed with organic soil according to our interpretation for Layer 9e; (b) To monitor the temperatures of the fire and in the interior of the structure, an analogic pyrometer model Silex Cr-Al 48.09 mV was used. The fire was produced on the structure using wood from rock rose branches and roots, as well as grasses in the ignition process, thus simulating the interpretations made from the study of the coals found in Layer 9; (c) The covering crust was then broken and removed with the aid of a stick, in order to expose the mound of leaves; (d) As the aim is to find out whether this resin could give rise to a viscous adhesive material, we reduced the labdanum placing shell containers over embers, in this way slowly heating it below the boiling point; (e) In order to accelerate the process of polymerization and, at the same time, produce more volume of pitch, we mixed 2–3 g of ashes; (f) Spearheads using the Levallois technique were produced from a flint cobble for the purpose of the experiment, while the rockrose leaves were steaming in the kiln. With the pitch still hot and elastic, it was applied to adhere the spearhead to a handle made of wild olive *Olea europaea* var. *sylvestris*; (g) Detail of the obtained hafted Levallois spearhead.

We conclude that it is possible to obtain tar in appreciable quantities by rapid manual pressing (Figs. S35–S67). From less than 2 kg of young rockrose leaves 100 ml of tar was obtained, enough for hafting at least two spearheads (Fig. 7 and S60-S67). The use of pyrotechnology is common among aboriginal Australians in order to produce resins from herbaceous plants (Bradshaw, 2013). *Spinifex* resin is known to have been used as a handling adhesive to make composite tools such as spears and to attach handles to a variety of tools and weapons (Pitman and Wallis, 2012). Among modern humans the oldest evidence of adhesives is back to the African Middle Stone Age (Kozowyk et al., 2023).

5.5. Experiments developed to analyze the potentialities of Cistus ladanifer to produce tar based in the structure found in Vanguard Cave (Layer 10)

We find size and morphological similarities between the Vanguard Cave Layer 10 hearth and the concave pit hearths from Level O at Abric Romaní and Pech d l'Azé Nord site, including small dug trenches to control airflow (Vallverdú et al., 2012; Courty et al., 2012). These similarities and the different combustion structures found in Abric Romaní indicate different uses of fire given by Neanderthals. The development of a "kiln-like" sediment mound over the pit to produce the dry distillation of the rockrose leaves, following (Groom et al., 2015), is not clear in the Layer 10 structure of Vanguard Cave; however, there is enough evidences for sediment thermal alteration, including the "lining" or crust made of hardened sediment that is found in some parts of the structure. We assume that just the sealing of the pit with a cover of moistened sediment would be enough to place the fire immediately over it and obtain the same results as we did in the experiments, but producing less quantity of pitch since the quantity of leaves required to fill completely the pit would be smaller.

Birch and conifers are the best-known resins to have been used to produce tar by Neanderthals (Mazza et al., 2006; Niekus et al., 2019; Kozowyk et al., 2017; Rageot et al., 2018; Degano et al., 2019). No doubt *Cistus ladanifer*, or rockrose, has been collected to kindle fires since it shows a very hard and highly inflammable wood. Labdanum is a resin impregnating the leaves of rockrose whose strong adhesion can be empirically perceived by collecting the plant, especially the young leaves. Rockrose is typical from very poor, immature soils, being common in the coastal rocky areas and dunes from Andalucía, as well as the Central and South of Portugal (Morgado et al., 2005). Rockroses were also present in the landscape outside Vanguard Cave. In Extremadura and other regions of Spain, small black balls of labdanum tar called "*melojas*" were produced in the past by fast boiling of rockrose in caldrons and used by the perfume industry (Morgado et al., 2005; Martín et al., 2009).

Using simple techniques and tools, available to Neanderthals, we presented with our experiments the *chaîne opératoire* with the technical steps needed to produce tar from labdanum secreted by rockrose leaves in the scenario of hafting. Tar made of rockrose is a dark brown or black viscous liquid of hydrocarbons and free carbon, obtained through destructive distillation at low temperatures (<150 °C), without fully anoxic conditions. This tar produced from rockrose labdanum increases the viscosity to a solid pitch achieved when cold. In contact with air, it has similar characteristics to contact glue. Plant starches are natural polymers. The evaporation of water leads to the formation of a polymeric film, which will be responsible for the adhesive layer that holds two surfaces together. The application of ashes significantly accelerated the process of polymerization. The quantity of ashes used can also control the plasticity of the tar in order to be molded around stone tools. After being cooked, cooled and solidified, tar could be reheated to soften again. We managed to produce a significant amount of tar in a relevant period of time of not more than 4 h, counting from collecting wood to hafting.

Certainly, some form of container would be necessary to cook the pitch. We used bivalve shells since they are common in the stratigraphic succession of the Vanguard Cave (Stringer et al., 2008) and were most likely transported by Neanderthals. They are usually found highly fragmented, although no study was performed yet to understand if this fragmentation resulted from being cooked under the fire or *for cooking* under direct fire.

6. Conclusion

Neanderthals were able to construct layered and complex hearths with specific technological objectives that could have included tool, medicine and/or weapon elaboration. At the Vanguard Cave of Gibraltar, in layers geochronologically well constrained between 67.6 ± 5.3 ka to 60.8 ± 11.0 ka, we identify for the first time a Neanderthal's specialised burning structure compatible with essential oils steam distillation from rockroses (Cistaceae) for tar production, based on the following evidence.

- A hearth with unusual morphological features, clearly anthropogenic, composed of a central, almost circular pit with two opposite sided trenches opened according to the orientation of the cave and following the air circulation patterns, revealing a crust of altered sediment by pyrometamorphism;
- BPCA analysis confirmed the abundance of pyrogenic materials in all analysed layers. The relatively uniform B5CA/B6CA ratio (ca. 0.7–1) indicates a similar degree of pyrolysis for all samples, suggesting that they were originated from similar thermal/pyrolytic processes;
- FTIR results indicate that analysed clays minerals within the structure show no evidence of clay heating >500 °C, showing structure infilling by a mix of *in situ* (combusted) and lateral (unalterated) sediments; the presence of carbonate rocks within the structure are interpreted as anthropogenic and used for sustaining the sealing made of guano and sand;
- While most detritic-rich sediment in VC is palynologically sterile, the structure itself was rich in pollen grains, which suggests anthropogenic introduction of pollen-derived plants. Sealing of the structure creating an anoxic environment, and low temperature baking, explain the preservation of pollen inside the structure;
- The presence of levoglucosan and especially large amounts of retene in the structure's matrix points to combustion of higher resinous plant-derived material;
- Lipid compounds were analysed, showing straight-chain n-alkanes of odd carbon number and n-alkanols of even carbon number, biomarkers highly conserved as fresh leaf wax;
- Based on charcoal analysis specimens of Cistaceae have been found partially vitrified, or incompletely burned, with <10% of conifer wood;
- Experimental tar samples were dominated by irregular isotropic crystals with a bright yellow colour similar to the ones recognized under the microscopic at layer 9, with enabled identifying them as urea or resin crystals.

The hearth structure coincides with predictions from theoretical studies on birch tar which require the use of heating structures for obtaining tar, a hafting substance that was proved to be used by Neanderthals. Our interpretations were experimentally tested by building a structure with morphological and compositional features analogous to the one excavated in VC. Distilling a small bunch of young leaves of rockrose for a reasonable period of time in a closed and almost anoxic environment enabled to produce tar that was more than enough to haft two spearheads, using only tools and materials available in the area for the period in reference. And following the cognitive reasoning and *chaîne opératoire* that were most logically developed by Neanderthals.

CRediT authorship contribution statement

Juan Ochando: Conceptualization, Data curation, Formal analysis,

Investigation, Methodology, Software, Writing – original draft. **Francisco J. Jiménez-Espejo:** Conceptualization, Data curation, Formal analysis, Investigation, Methodology, Software, Writing – original draft. **Francisco Giles-Guzmán:** Conceptualization, Data curation, Formal analysis, Investigation, Methodology, Software, Writing – original draft. **Carlos Neto de Carvalho:** Investigation, Methodology, Software, Writing – original draft. **Jose S. Carrión:** Funding acquisition, Investigation, Methodology, Project administration, Resources, Supervision, Validation. **Fernando Muñiz:** Investigation, Software, Supervision. **Juan Manuel Rubiales:** Investigation, Methodology, Supervision, Validation, Writing – review & editing. **Pedro Cura:** Investigation, Methodology, Supervision, Validation, Writing – review & editing. **João Belo:** Investigation, Methodology, Supervision, Validation, Writing – review & editing. **Stewart Finlayson:** Project administration, Resources, Supervision. **Belen Martrat:** Investigation, Methodology, Supervision, Validation, Writing – review & editing. **Barend L. van Drooge:** Investigation, Software, Supervision. **Gonzalo Jiménez-Moreno:** Investigation, Software, Supervision. **Antonio García-Alix:** Investigation, Methodology, Supervision, Validation, Writing – review & editing. **Jose Antonio Lozano Rodríguez:** Investigation, Software, Supervision. **Rosa María Albert:** Investigation, Methodology, Supervision, Validation, Writing – review & editing. **Naohiko Ohkouchi:** Investigation, Methodology, Supervision, Validation, Writing – review & editing. **Nanako Ogawa:** Investigation, Methodology, Supervision, Validation, Writing – review & editing. **Hisami Suga:** Investigation, Methodology, Supervision, Validation, Writing – review & editing. **Jon Camuera:** Investigation, Software, Supervision. **Francisca Martínez-Ruiz:** Investigation, Methodology, Supervision, Validation, Writing – review & editing. **Joan Villanueva:** Investigation, Methodology, Supervision, Validation, Writing – review & editing. **Oriol Teruel:** Investigation, Software, Supervision. **Nina Davtian:** Investigation, Software, Supervision. **Noel Moreira:** Investigation, Software, Supervision. **Zain Belaústegui:** Investigation, Software, Supervision. **Joaquín Rodríguez-Vidal:** Investigation, Methodology, Supervision, Validation, Writing – review & editing. **Manuel Munuera:** Investigation, Software, Supervision. **Alex Menez:** Project administration, Resources, Supervision. **Geraldine Finlayson:** Project administration, Resources, Supervision. **Clive Finlayson:** Conceptualization, Funding acquisition, Investigation, Methodology, Project administration, Resources, Supervision, Validation, Writing – review & editing.

Declaration of competing interest

The authors declare that they have no known competing financial interests or personal relationships that could have appeared to influence the work reported in this paper.

Acknowledgments and Funding

The development of this work was supported by Projects CGL-BOS2015-68604-P, PID2019-1049449 GB-I00, HOMEDSCAPE, PID2022-136832NB-100, PID2020-119773 GB-I00 Ministerio de Ciencia e Innovación, Spain and PID2021-125619OB-C21/C22 funded by FEDER/Ministry of Science and Innovation, Agencia Estatal de Investigación, Fundación Séneca (grant no. 20788/PI/18) and Proyecto LifeWatch ERIC-SUMHAL, LIFEWATCH-2019-09-CSIC-13. JMR would like to thank Victoria Fernández (UPM) for making possible the SEM observations in brief delays, as well as Miriam González from the ICTS-CNME, for her kind work under difficult conditions due to the sanitary restrictions. BM was funded by the CSIC Ramón y Cajal postdoctoral programme RYC-2013-14073, LINKA20102 and the Spanish Ministry of Science and Innovation projects CEX2018-000794-S and PID2022-137665NB-I00 AEI/10.13039/501100011033/FEDER, UE. NP, OT, and JV are supported by Secretariat of Universities and Research of Catalonia [FI-DGR grant 2019FI-B00522] and "María de Maeztu" Programme of the Spanish Ministry of Science and Innovation [CEX2019-000940-M]. N. Moreira (ICT) is financed by FCT - Fundação para a Ciência e a Tecnologia, I.P., under the project Ref. UIDB/04683/2020. Thank to Celia Roldán Alaminos for the artistic recreation included in Fig. 6.

Appendix A. Supplementary data

Supplementary data to this article can be found online at https://doi.org/10.1016/j.quascirev.2024.109025.

Data availability

Data will be made available on request.

References

Agam, A., Azuri, I., Pinkas, I., Gopher, A., Natalio, F., 2021. Estimating temperatures of heated lower palaeolithic flint artefacts. Nat. Human Behav. 5, 221–228.

Allen, J.R., 1997. Subfossil mammalian tracks (Flandrian) in the Severn Estuary, SW Britain: mechanics of formation, preservation and distribution. Philos. Trans. R. Soc. 352, 481–518.

Allué, E., Solé, A., Burguet-Coca, A., 2017. Fuel exploitation among Neanderthals based on the anthracological record from abric Romaní (Capellades, NE Spain). Quat. Int. 431, 6–15.

Aranguren, B., Revedin, A., Amico, N., Cavulli, F., Giachi, G., Grimaldi, S., Macchioni, N., Santaniello, F., 2018. Wooden tools and fire technology in the early Neanderthal site of Poggetti Vecchi (Italy). Proc. Natl. Acad. Sci. U. S. A 115, 2054–2059.

Bea, F., 1996. Controls on the trace element composition of crustal melts. Earth Environ. Sci. Trans. R. Soc. Edinb 87, 33–41.

Berna, F., Behar, A., Shahack-Gross, R., Berg, J., Boaretto, E., Gilboa, A., Sharon, I., Shalev, S., Shilstein, S., Yahalom-Mack, N., Zorn, J.R., Weiner, S., 2007. Sediments exposed to high temperatures: reconstructing pyrotechnological processes in late bronze and iron age strata at tel dor (Israel). J. Archaeol. Sci. 34, 358–373.

Bertling, M., Braddy, S.J., Bromley, R.G., Demathieu, G.R., Genise, J., Mikuláš, R., Nielsen, J.K., Nielsen, K.S.S., Rindsberg, A.K., Schlirf, M., Uchman, A., 2007. Names for trace fossils: a uniform approach. Lethaia 39, 265–286.

Boëda, E., Bonilauri, S., Connan, J., Jarvie, D., Mercier, N., Tobey, M., Valladas, H., al Sakhel, H., Muhesen, S., 2008. Middle Palaeolithic bitumen use at Umm el Tlel around 70 000 BP. Antiquity 82, 853–861.

Bradshaw, F., 2013. Chemical characterisation of museum-curated ethnographic resins from Australia and New Guinea used as adhesives, medicines and narcotics. Herit. Sci. 1, 36.

Brown, K.S., Marean, C.W., Herries, A.I.R., Jacobs, Z., Tribolo, C., Braun, D., Roberts, D. L., Meyer, M.C., Bernatchez, J., 2009. Fire as an engineering tool of early modern humans. Science 325, 859–862.

Buatois, L.A., Mángano, M.G., 2011. Ichnology. Organism-Substrate Interactions in Space and Time. Cambridge University Press.

Burger, L., 2016. Investigação e comparação de metodologias de extração de lábdano obtido a partir de *Cistus ladanifer* L. Instituto Politécnico de Bragança and University of Salamanca.

Carrión, J.S., Scott, L., 1999. The challenge of pollen analysis in palaeoenvironmental studies of hominid beds. the record from Sterkfontein Caves. J. Hum. Evol. 36, 401–408.

Carrión, J.S., Scott, L., Huffman, T., Dreyer, C., 2000. Pollen analysis of Iron Age cow dung in southern Africa. Veg. Hist. Archaeobotany 9, 239–249.

Carrión, J.S., Finlayson, C., Fernández, S., Finlayson, G., Allué, E., López-Sáez, A., López-García, P., Fuentes, N., Gil, G., González-Sampériz, P., 2008. A coastal reservoir of biodiversity for Upper Pleistocene human populations: palaeoecological investigations in Gorham's Cave (Gibraltar) in the context of the Iberian Peninsula. Quat. Sci. Rev. 27, 2118–2135.

Carrión, J.S., Fernández, S., González-Sampériz, P., Leroy, S.A.G., López-Sáez, J.A., Burjachs, F., Gil-Romera, G., Rodríguez-Sánchez, E., García-Antón, M., Gil-García, M.J., Parra, I., Santos, L., López-García, P., Yll, E.I., Dupré, M., 2009. Sterility cases and causes in Quaternary pollen analysis in the Iberian Peninsula: the advantages of reporting bad luck. Internet Archaeol. 25, 1–54. http://intarch.ac.uk/journal/issue25/5/toc.html.

Carrión, J.S., Ochando, J., Fernández, S., Munuera, M., Amorós, G., Blasco, R., Rosell, J., Finlayson, S., Giles, F., Jennings, R., Finlayson, G., Giles-Pacheco, F., Rodríguez-Vidal, J., Finlayson, C., 2018. Last Neanderthals in the warmest refugium of Europe: palynological data from Vanguard Cave. Review of Palaeobotany and Palynology, Special Issue (Carrión, J. S., deMenocal, P., Scott, L., eds.): human evolution and palaeofloras: the contribution and potential of palaeobotany in the environmental reconstruction of hominin-bearing sites. Rev. Palaeobot. Palynol. 259, 63–80.

Chabal, L., et al., 1999. In: Bourquin-Mignot, C., Brochier, J.E., Chabal, L., Crozat, S., Fabre, L., Guibal, F., Marinval, P., Richard, H., Terral, J.F., Théry-Parisot, I. (Eds.), L'anthracologie in *La Botanique*. Errance, Paris.

Courty, M.A., Carbonell, E., Vallverdú Poch, J., Banerjee, R., 2012. Microstratigraphic and multi-analytical evidence for advanced Neanderthal pyrotechnology at Abric Romani (Capellades, Spain). Quat. Int. 247, 294–312.

Davtian, N., Penalva, N., Rosell-Melé, A., Villanueva, J., 2023. Selective extraction of levoglucosan and its isomers from complex matrices using ligand exchange-solid

phase extraction for analysis by liquid chromatography-electrospray ionization-tandem mass spectrometry. J. Chromatogr. A 1695, 463935.
Degano, I., Soriano, S., Villa, P., Pollarolo, L., Lucejko, J.J., Jacobs, Z., Douka, K., Vitagliano, S., Tozzi, C., 2019. Hafting of middle paleolithic tools in latium (central Italy): new data from fossellone and Sant'Agostino caves. PLoS One 14, e0213473.
Dimbleby, G.W., 1985. The Palynology of Archaeological Sites. Academic Press, London.
Doerschner, N., Fitzsimmons, K.E., Blasco, R., Finlayson, G., Rodríguez-Vidal, J., Rosell, J., Hublin, J.-J., Finlayson, C., 2019. Chronology of the Late Pleistocene archaeological sequence at Vanguard Cave, Gibraltar: insights from quartz single and multiple grain luminescence dating. Quat. Int. 501, 289–302.
Eglinton, T.I., Eglinton, G., 2008. Molecular proxies for paleoclimatology. Earth Planet Sci. Lett. 275, 1–16.
Erdtman, G., 1969. Handbook of Palynology. Hafner Publishing Company, Nueva York.
Frazão, D.F., Raimundo, J.R., Domingues, J.L., Quintela-Sabarís, C., Gonçalves, J.C., Delgado, F., 2018. *Cistus ladanifer* (Cistaceae): a natural resource in Mediterranean-type ecosystems. Planta 247, 289–300.
Girard, M., 1975. Prévèlement d'échantillons en grotte et station de terrain sec en vue de l'analyse pollinique. Bull. de la Soc. Prehis. Française 72, 158–160.
Girard, M., Renault-Miskovsky, J., 1969. Nouvelles techniques de preparation en palynologie appliques a trois sediments du Quaternaire final de l'Abri Corneille (Istres-Bouches-du-Rhone). Bull. Assoc. Fr. Etude Quat. 4, 275–284.
Godffrey, G.K., 1955. A field study of the activity of the mole (Talpa europaea). Ecology 678–685.
Greguss, P., 1955. Identification of living gymnosperms on the basis of xylotomy. Akademiai Kiadó, Budapest. Hungary.
Groom, P., Schenck, T., Pedersen, G.M., 2015. Experimental explorations into the aceramic dry distillation. Archaeol. Anthropol. Sci. 7, 47–58.
Grünberg, J.M., 2002. Middle Palaeolithic birch-bark pitch. Antiquity 76, 15–16.
Henry, A.G., 2017. Neanderthal cooking and the costs of fire. Curr. Anthropol. 58, S329–S336.
Heyes, P.J., Anastasakis, K., de Jong, W., van Hoesel, A., Roebroeks, W., Soressi, M., 2016. Selection and use of manganese dioxide by Neanderthals. Sci. Rep. 6, 22159.
Hoch, A.R., Reddy, M.M., Aiken, G.R., 2000. Calcite crystal growth inhibition by humic substances with emphasis on hydrophobic acids from the Florida Everglades. Geochem. Cosmochim. Acta 64, 61–72.
Jiménez-Espejo, F.J., Rodríguez-Vidal, J., Finlayson, C., Martínez-Ruiz, F., Carrión, J.S., García-Alix, A., Paytan, A., Giles Pacheco, F., Fa, D.A., Finlayson, G., Cortés-Sánchez, M., Rodrigo, Gámiz M., González-Donoso, J.M., Dolores Linares, M., Cáceres, L.M., Fernández, S., Lijima, K., Martínez Aguirre, A., 2013. Environmental conditions and geomorphologic changes during the middle-upper paleolithic in the southern iberian Peninsula. Geomorphology 180–181, 205–216.
Jurczyszyn, M., 2007. Hibernation cavities used by the edible dormouse, *glis Glis* (Gliridae, Rodentia). Folia Zool. 56, 162–168.
Karkanas, P., 2021. All about wood ash: long term fire experiments reveal unknown aspects of the formation and preservation of ash with critical implications on the emergence and use of fire in the past. J. Archaeol. Sci. 135, 105476.
Katz, O., Cabanes, D., Weiner, S., Maeir, A.M., Boaretto, E., Shahack-Gross, R., 2010. Rapid phytolith extraction for analysis of phytolith concentrations and assemblages during an excavation: an application at Tell es-Safi/Gath, Israel. J. Archaeol. Sci. 37, 1557–1563.
Kohn, M.J., 2010. Carbon isotope compositions of terrestrial C3 plants as indicators of (paleo) ecology and (paleo) climate. Proc. Natl. Acad. Sci. U. S. A 107, 19691–19695.
Kolb, H.H., 1985. The burrow structure of the European rabbit (Oryctolagus cuniculus L.). J. Zool. 206, 253–262.
Kolb, H.H., 1991. Use of burrows and movements by wild rabbits (Oryctolagus cuniculus) on an area of sand dunes. J. Appl. Ecol. 879–891.
Koller, J., Baumer, U., Mania, D., 2001. High-tech in the middle palaeolithic: Neandertal-manufactured pitch identified. Eur. J. Archaeol. 4, 385–397.
Kozowyk, P.R.B., Soressi, M., Pomstra, D., Langejans, G.H.J., 2017. Experimental methods for the Palaeolithic dry distillation of birch bark: implications for the origin and development of Neandertal adhesive technology. Sci. Rep. 7, 1–9.
Kozowyk, P.R.B., Baron, L.I., Langejans, G.H., 2023. Identifying Palaeolithic birch tar production techniques: challenges from an experimental biomolecular approach. Sci. Rep. 13, 14727.
Leierer, L., Alonso, Á.C., Pérez, L., Lagunilla, Á.H., Herrera-Herrera, A.V., Connolly, R., Jambrina Enríquez, M., Hernández Gómez, C.M., Galván, B., Mallol, C., 2020. It's getting hot in here – Microcontextual study of a potential pit hearth at the Middle Paleolithic site of El Salt, Spain. J. Archaeol. Sci. 123, 105237.
Macphail, R.I., Goldberg, P., 2000. Geoarchaeological investigation of sediments from Gorham's and Vanguard Caves, Gibraltar: microstratigraphical (soil micromorphological and chemical) signatures. In: Stringer, C.B., Barton, R.N.E., Finlayson, J.C. (Eds.), Neanderthals on the Edge. Oxbow Books, Oxford, pp. 183–200.
Macphail, R.I., Goldberg, P., Barton, R.N.E., 2013. Vanguard Cave sediments and soil micromorphology. In: Barton, R.N.E., Stringer, C.B., Finlayson, J.C. (Eds.), Neanderthals in Context. A Report of the 1995-1998 Excavations at Gorham's and Vanguard Caves, Gibraltar. Oxford University School of Archaeology, pp. 193–210.
Marais, E., Scott, L., Gil-Romera, G., Carrion, J.S., 2015. The potential of palynology in fossil bat-dung from Arnhem Cave, Namibia. Trans. Roy. Soc. S. Afr. 70, 109–115.
Martín, J.M.C., Cardenal Galván, J.A., Peral Pacheco, D., Vallejo Villalobos, J.R., 2009. Jara pringosa (*Cistus ladanifer*): usos, utilidades y curiosidades en Extremadura. Revista de Estudos Extremeños 65 (III), 1637–1650.
Mazza, P.P.A., Martini, F., Sala, B., Magi, M., Colombini, M.P., Giachi, G., Landucci, F., Lemorini, C., Modugno, F., Ribechini, E., 2006. A new Palaeolithic discovery: tar-hafted stone tools in a European Mid-Pleistocene bone-bearing bed. J. Archaeol. Sci. 33, 1310–1318.
Medeiros, P.M., Simoneit, B.R.T., 2007. Analysis of sugars in environmental samples by gas chromatography–mass spectrometry. J. Chromatogr. A 1141, 271–278.
Milàn, J., Bromley, R.G., 2006. True tracks, undertracks and eroded tracks, experimental work with tetrapod tracks in laboratory and field. Palaeogeogr. Palaeoclimatol. Palaeoecol. 231, 253–264.
Modugno, F., Ribechini, E., Colombini, M.P., 2006. Chemical study of triterpenoid resinous materials in archaeological findings by means of direct exposure electron ionisation mass spectrometry and gas chromatography/mass spectrometry. Rapid Commun. Mass Spectrom. 20, 1787–1800.
Monge, G., Jimenez-Espejo, F.J., García-Alix, A., Martínez-Ruiz, F., Marrielli, N., Finlayson, C., Ohkouchi, N., Cortés Sánchez, M., Bermúdez de Castro, J.M., Blasco, R., Rosell, J., Carrión, J.S., Rodríguez-Vidal, J., Finlayson, G., 2015. Earliest evidence of pollution by heavy metals in archaeological sites. Sci. Rep. 5, 1–9.
Moretti, M., Conedera, M., Moresi, R., Guisan, A., 2006. Modelling the influence of change in fire regime on the local distribution of a mediterranean pyrophytic plant species (*Cistus salviifolius*) at its northern range limit. Wiley 33, 1492–1502.
Morgado, J.M., Tapias, R., Alesso, P., 2005. Producción de Goma Bruta de Jara (*Cistus ladanifer* L.) en el Suroeste de la Península Ibérica. Universidad de Huelva.
Niekus, M.J.L.Th, Kozowyk, P.R.B., Langejans, G.H.J., Ngan-Tillard, D., van Keulen, H., van der Plicht, J., Cohen, K.M., van Wingerden, W., van Os, B., Smit, B.I., Amkreutz, L.W.S.W., Johansen, L., Verbaas, A., Dusseldorp, G.L., 2019. Middle paleolithic complex technology and a neandertal tar-backed tool from the Dutch north sea. Proc. Natl. Acad. Sci. U. S. A 116, 22081–22087.
Pawlik, A.F., Thissen, J.P., 2011. Hafted armatures and multi-component tool design at the Micoquian site of Inden-Altdorf, Germany. J. Archaeol. Sci. 38, 1699–1708.
Pelletier, M., Brugal, J.P., Cochard, D., Lenoble, A., Mallye, J.B., Royer, A., 2016. Identifying fossil rabbit warrens: insights from a taphonomical analysis of a modern warren. J. Archaeol. Sci. 10, 331–344.
Pelletier, M., Royer, A., Holliday, T.W., Discamps, E., Madelaine, S., Maureille, B., 2017. Rabbits in the grave! Consequences of bioturbation on the neandertal "burial" at regourdou (Montignac-sur-Vézère, dordogne). J. Hum. Evol. 110, 1–17.
Pettitt, P.B., Bailey, R.M., 2000. AMS radiocarbon and luminescence dating of Gorham's and vanguard caves, Gibraltar, and implications for the Middle to upper palaeolithic transition in Iberia. In: Stringer, C.B., Barton, R.N.E., Finlayson, J.C. (Eds.), Neanderthals on the Edge. Oxbow Books, Oxford, pp. 155–162.
Pitman, H., Wallis, L., 2012. The point of Spinifex: aboriginal uses of spinifex grasses in Australia. Ethnobot. Res. Appl. 10, 109–131.
Rageot, M., Rageot, M., Théry-Parisot, I., Beyries, S., Lepère, C., Carré, A., Mazuy, A., Filippi, J.-J., Fernandez, X., Binder, D., Regert, M., 2018. Birch bark tar production: experimental and biomolecular approaches to the study of a common and widely used prehistoric adhesive. J. Archaeol. Method Theor 26, 276–312.
Regev, L., Regev, L., Poduska, K.M., Addadi, L., Weiner, S., Boaretto, E., 2010. Distinguishing between calcites formed by different mechanisms using infrared spectrometry: archaeological applications. J. Archaeol. Sci. 37, 3022–3029.
Rodríguez-Vidal, J., Finlayson, G., Finlayson, C., Negro, J.J., Cáceres, L.M., Fa, D.A., Carrión, J.S., 2013. Undrowning a lost world - the marine isotope stage 3 landscape of Gibraltar. Geomorphology 203, 105–114.
Roebroeks, W., Villa, P., 2011. On the earliest evidence for habitual use of fire in Europe. Proc. Natl. Acad. Sci. U.S.A. 108, 5209–5214.
Rosell, J., Blasco, R., 2019. The early use of fire among Neanderthals from a zooarchaeological perspective. Quat. Sci. Rev. 217, 268–283.
Rots, V., Hayes, E., Akerman, K., Green, P., Clarkson, C., Lepers, C., Bordes, L., McAdams, C., Foley, E., Fullagar, R., 2020. Hafted tool-use experiments with Australian aboriginal plant adhesives: Triodia spinifex, Xanthorrhoea grass tree and Lechenaultia divaricata Mindrie. Exarc J. https://exarc.net/ark:/88735/10487.
Sankararaman, S., Mallick, S., Dannemann, M., Prüfer, K., Kelso, J., Pääbo, S., Patterson, N., Reich, D., 2014. The genomic landscape of Neanderthal ancestry in present-day humans. Nature 507, 354–357.
Schweingruber, F., 1990. Anatomy of European Woods. Stuttgart, WSL/FNP, Paul Haupt. Stuttgart Publishers, Berne.
Schmidt, P., Blessing, M., Rageot, M., Iovita, R., Pfleging, J., Nickel, K.G., Righetti, L., Tennie, C., 2019. Birch tar production does not prove Neanderthal behavioral complexity. Proc. Natl. Acad. Sci. U.S.A. 116, 17707–17711.
Schmidt, P., Koch, T.J., Blessing, M.A., Karakostis, F.A., Harvati, K., Dresely, V., Charrié-Duhaut, A., 2023. Production method of the Königsaue birch tar documents cumulative culture in Neanderthals. Archaeol. Anthropol. Sci. 15, 84.
Schmidt, P., Iovita, R., Charrié-Duhaut, A., Möller, G., Namen, A., Dutkiewicz, E., 2024. Ochre-based compound adhesives at the Mousterian type-site document complex cognition and high investment. Sci. Adv. 10, eadl0822.
Simoneit, B.R.T., 1977. Diterpenoid compounds and other lipids in deep-sea sediments and their geochemical significance. Geochem. Cosmochim. Acta 41, 463–473.
Sorensen, A.C., Claud, E., Soressi, M., 2018. Neandertal fire-making technology inferred from microwear analysis. Sci. Rep. 8, 10065.
Stringer, C.B., Finlayson, C., Barton, R.N.E., Fernández-Jalvo, Y., Cáceres, I., Sabin, R.C., Rhodes, E.J., Currant, A.P., Rodríguez-Vidal, J., Giles-Pacheco, F., Riquelme-Cantal, J.A., 2008. Neanderthal Exploitation of marine mammals in Gibraltar. Proc. Natl. Acad. Sci. U. S. A 105, 14319–14324.
Théry-Parisot, I., 2001. Économie des combustibles au Paléolithique: expérimentation, taphonomie, anthracologie. In: Dossier de Documentation Archéologique 20. CNRS Éditions, Paris.
Théry-Parisot, I., Meignen, L., 2000. Économie des combustibles (bois et lignite) dans l'abri Moustérien des Canalettes [l'expérimentation à la simulation des besoins énergétiques]. Gall. Prehist. 42, 45–55.

Uzquiano, P., 2008. Domestic fires and vegetation cover among Neanderthalians and anatomically modern human groups (>53e30 Kyrs. BP) in the Cantabrian region (Cantabria, Northern Spain). In: Fiorentino, G., Magri, D. (Eds.), Charcoal from the Past: Cultural and Palaeoenvironmental Implications, vol. 1807. B.A.R. International Series, Oxford, UK, p. 273e285.

Vallverdú, J., Alonso, S., Bargalló, A., Bartrolí, R., Campeny, G., Carrancho, Á., Expósito, I., Fontanals, M., Gabucio, J., Gómez, B., Prats, J.M., Sañudo, P., Solé, À., Vilalta, J., Carbonell, E., 2012. Combustion structures of archaeological level O and Mousterian activity areas with use of fire at the Abric Romaní rockshelter (NE Iberian Peninsula). Quat. Int. 247, 313–324.

Vernet, J.L., Ogereau, P., Figueiral, I., Machado Yanes, C., Uzquiano, P., 2001. Guide d'identification des charbons de bois préhistoriques et récents du Sud-Ouest de l'Europe, France. In: Péninsule ibérique et Îles Canaries. CNRS Editions, Paris.

Vidal-Matutano, P., Théry-Parisot, I., 2016. The earliest evidence of a smoking hearth? A palaeoeconomical approach from el salt (Eastern Iberia). In: Proceedings of the 6th Annual ESHE Meeting, Madrid (Spain).

Vidal-Matutano, P., Blasco, R., Sañudo, P., Fernández Peris, J., 2017. The anthropogenic use of firewood during the European middle Pleistocene: charcoal evidence from levels XIII and XI of Bolomor cave, Eastern Iberia (230–160 ka). Environ. Archaeol. 24, 1–16.

Weiner, S., 2010. In: Microarchaeology. Beyond the Visible Archaeological Record. Cambridge University Press.

Wilkins, J., Schoville, B.J., Brown, K.S., Chazan, M., 2012. Evidence for early hafted hunting technology. Science 338, 942.

Wöstehoff, L., Kindermann, K., Amelung, W., Kappenberg, A., Henselowsky, F., Lehndorff, E., 2022. Anthropogenic fire fingerprints in late Pleistocene and holocene sediments of Sodmein cave, Egypt. J. Archaeol. Sci. Rep 42, 103411.

Wrangham, R., 2009. Catching Fire: How Cooking Made Us Human. Basic Books, New York, NY.

Yravedra, J., Uzquiano, P., 2013. Burnt bone assemblages from El Esquilleu cave (Cantabria, Northern Spain). Deliberate use for fuel or systematic disposal of organic waste. Quat. Sci. Rev. 68, 175–190.